# RALGDS-DEPENDENT CARDIOMYOCYTE AUTOPHAGY IS NECESSARY FOR LOAD-INDUCED VENTRICULAR HYPERTROPHY

APPROVED BY SUPERVISORY COMMITTEE

Joseph A. Hill, M.D., Ph.D. (Mentor)

Michael A. White, Ph.D. (Chair)

Beth Levine, M.D.

Eric N. Olson, Ph.D.

## Dedication

I would like to thank Dr. Richard M. Weinshilboum, my first scientific mentor during my SURF at the Mayo Clinic. He truly set my scientific career in motion. Also Dr. Urs A. Meyer, my mentor during my Fulbright fellowship at the University of Basel, was instrumental in furthering my scientific progress.

Thank you to Dr. Joseph A. Hill for his balance of patience, encouragement and prodding in guiding me through my thesis work. I will continue to model my career as a physician-scientist upon his example and know that I can always look to him for guidance and support.

Thank you of course to my family. My father, Dr. Fatih A. Rifki, who taught me early the beauty of academia and shared his passion for never stopping learning. My mother, Hatice F. Rifki, taught me the importance of compassion and the beauty of caring for others. My brother, Ahmet F. Rifki, has been my friend and companion through out it all, helping to keep me grounded.

# RALGDS-DEPENDENT CARDIOMYOCYTE AUTOPHAGY IS NECESSARY FOR LOAD-INDUCED VENTRICULAR HYPERTROPHY

by

OKTAY FERIDUN RIFKI

DISSERTATION

Presented to the Faculty of the Graduate School of Biomedical Sciences

The University of Texas Southwestern Medical Center at Dallas

In Partial Fulfillment of the Requirements

For the Degree of

DOCTOR OF PHILOSOPHY

The University of Texas Southwestern Medical Center at Dallas

Dallas, TX

May 2014

# RALGDS-DEPENDENT CARDIOMYOCYTE AUTOPHAGY IS NECESSARY FOR LOAD-INDUCED VENTRICULAR HYPERTROPHY

OKTAY FERIDUN RIFKI

The University of Texas Southwestern Medical Center at Dallas, 2014

JOSEPH A. HILL, M.D., Ph.D.

Recent work has demonstrated that autophagy, a phylogenetically conserved, lysosome-mediated pathway of protein degradation, is a key participant in pathological cardiac remodeling. One common feature of cell growth and autophagy is membrane biogenesis and processing. The exocyst, an

octomeric protein complex involved in vesicle trafficking, is implicated in numerous cellular processes, yet its role in cardiomyocyte plasticity is unknown. Here, I set out to explore the role of small G protein-dependent membrane trafficking in stress-induced cardiomyocyte remodeling and autophagy. To explore underlying mechanisms, I tested in cultured neonatal cardiomyocytes two isoforms of Ral that are downstream of RalGDS (RalA, RalB) and whose actions are mediated by the exocyst. In these experiments, mTOR inhibition was maintained in response to starvation and Torin 1 despite RalA or RalB knockdown; however, autophagy was diminished only in NRCM's with RalB knockdown, implicating RalB as required for cardiomyocyte autophagy. Hearts from mice lacking RalGDS (*Ralgds*$^{-/-}$), a guanine exchange factor (GEF) for the Ral family of small GTPases, were similar to wild-type (WT) littermates in terms of ventricular structure, contractile performance, and gene expression. However, *Ralgds*$^{-/-}$ hearts manifested a blunted growth response ($p<0.05$) to TAC-mediated pressure-overload stress as determined by heart weight to body weight ratios Ventricular chamber size and contractile performance were preserved in response to TAC in *Ralgds*$^{-/-}$ mice. Interestingly, TAC-induced activation of the fetal gene program was similar in both genotypes despite the relative lack of hypertrophic growth in mutant hearts. *Ralgds*$^{-/-}$ mice also exhibited diminished load-induced cardiomyocyte autophagy. Consistent with the TAC findings, *Ralgds*$^{-/-}$ mice manifested a blunted autophagic response to 24-hour fasting, suggesting a generalized defect in autophagy. Together, these data implicate

RalGDS-mediated induction of autophagy as a critical feature of load-induced cardiac hypertrophy.

# Table of Contents

**Table of Contents** ..... **vii**
**Prior Publications** ..... **xi**
**List of Figures** ..... **xii**
**Chapter 1** ..... **13**
**Introduction** ..... **13**
Basal Autophagy ..... 16
Ischemia/Reperfusion Injury ..... 17
Hypertrophy and Failure ..... 21
Central Thesis ..... 24
**Chapter 2** ..... **26**
**Introduction** ..... **27**
**Materials & Methods** ..... **29**
Animal models and echocardiography ..... 29
Primary culture of neonatal cardiomyocytes, siRNA transfection and adenovirus infection ..... 29
Real-time RT-PCR ..... 30
Immunoblot analysis ..... 30
Histology ..... 31
Myocyte Cross-sectional Area ..... 31
Statistics ..... 31
**Results** ..... **32**
RalB is necessary for cardiomyocyte autophagy ..... 32
RalGDS is necessary for autophagy ..... 34

RalGDS$^{-/-}$ hearts manifested a blunted growth response and preserved function in response to pressure-overload stress ..... 36
RalGDS$^{-/-}$ mice exhibit diminished load-induced and starvation-induced cardiomyocyte autophagy ..... 37
**Discussion ..... 38**
RalGDS is an activator of cardiomyocyte autophagy ..... 38
RalGDS is necessary for cardiac hypertrophy in response to pressure-overload stress ..... 39
Cardiomyocyte autophagy is required for load-induced hypertrophy ..... 40
**Figures ..... 41**
**Chapter 3 ..... 55**
**Introduction ..... 56**
Anatomy of the mouse hind limb ..... 59
**Materials & Methods ..... 60**
Transgenic mice ..... 60
Histology ..... 61
Myocyte Fiber Cross-sectional Area ..... 61
Real-time RT-PCR ..... 61
Immunoblot analysis ..... 62
Statistics ..... 62
**Results ..... 63**
Transgenic mice, expressing constitutively active Foxo3a robustly and specifically in skeletal muscle are kyphotic, yet viable ..... 63
Atrophic response to Foxo3a overexpression is attenuated in muscle groups with more abundant oxidative fibers ..... 63

Overexpression of Foxo3a increases oxidative fibers ..... 64

Overexpression of Foxo3a induces atrogene, metabolic, & differentiation factors ..... 65

**Discussion ..... 67**
FoxO3a is an activator of skeletal muscle atrophy ..... 67

Oxidative skeletal muscle is resistant to atrophy ..... 68

Relevance ..... 69

**Figures ..... 70**
**Chapter 4 ..... 81**
**Introduction ..... 82**
**Materials & Methods ..... 83**
Mitochondrial dye incorporation ..... 83

Real-time RT-PCR ..... 84

Immunoblot analysis ..... 84

Transgenic mice ..... 85

Echocardiography ..... 85

Statistics ..... 85

**Results ..... 86**
Depolarized mitochondria are increased in phenylephrine induced hypertrophy ..... 86

Blocking autophagy attenuates the increase in depolarized mitochondria in response to phenylephrine ..... 87

Blocking autophagy attenuates mitochondrial fragmentation in response to PE treatment ..... 87

Phenylephrine treatment induces Drp1 phosphorylation at serine-616 ..... 88

Cre;Atg5$^{-/-}$ hearts show similar hypertrophy but diminished function in response to pressure-overload stress ..... 89

MCM;Atg5$^{f/f}$ hearts treated exhibit hypertrophy and diminished function in response to tamoxifen treatment ..... 90

**Discussion ..... 92**
**Figures ..... 94**
**Chapter 5 ..... 102**
Rationale ..... 103

RalGDS is essential for cardiomyocyte autophagy ..... 104

RalGDS is necessary for cardiac hypertrophy ..... 104

A role for RalGDS in physiological hypertrophy? ..... 105

Autophagy in skeletal muscle atrophy ..... 106

Oxidative skeletal muscle is resistant to atrophy ..... 106

Inconsistencies of mitophagy ..... 108

Modeling cardiac hypertrophy ..... 109

**Bibliography ..... 112**

## Prior Publications

Thomae BA, **Rifki OF**, Theobald MA, Eckloff BW, Wieben ED, Weinshilboum RM. Human catecholamine sulfotransferase (SULT1A3) pharmacogenetics: functional genetic polymorphism. *J Neurochem*. 2003 Nov;87(4):809-19.

Oscarson M, Zanger UM, **Rifki OF**, Klein K, Eichelbaum M, Meyer UA. Transcriptional profiling of genes induced in the livers of patients treated with carbamazepine. *Clin Pharmacol Ther*. 2006 Nov;80(5):440-456.

Moresi V, Carrer M, Grueter CE, **Rifki OF**, Shelton JM, Richardson JA, Bassel-Duby R, Olson EN. Histone deacetylases 1 and 2 regulate autophagy flux and skeletal muscle homeostasis in mice. *Proc Natl Acad Sci U S A*. 2012 Jan 31;109(5):1649-54.

## List of Figures


**Figure 2.1 A-B** ..... **41**
**Figure 2.1 C-D** ..... **42**
**Figure 2.1 E** ..... **43**
**Figure 2.1 F** ..... **44**
**Figure 2.2 A-B** ..... **45**
**Figure 2.2 C-D** ..... **46**
**Figure 2.2 E** ..... **47**
**Figure 2.2 F** ..... **48**
**Figure 2.3** ..... **49**
**Figure 2.4** ..... **50**
**Figure 2.5 A-B** ..... **51**
**Figure 2.5 C** ..... **52**
**Figure 2.6 A-C** ..... **53**
**Figure 2.6 D** ..... **54**
**Figure 3.1** ..... **70**
**Figure 3.2** ..... **71**
**Figure 3.3 A** ..... **72**
**Figure 3.3 B** ..... **73**
**Figure 3.3 C** ..... **74**
**Figure 3.3 D** ..... **75**
**Figure 3.3 E** ..... **76**
**Figure 3.4 A** ..... **77**
**Figure 3.4 B** ..... **78**
**Figure 3.5 A-C** ..... **79**
**Figure 3.5 D** ..... **80**
**Figure 4.1** ..... **94**
**Figure 4.2 A-B** ..... **95**
**Figure 4.2 C-D** ..... **96**
**Figure 4.3 A** ..... **97**
**Figure 4.3 B** ..... **98**
**Figure 4.4** ..... **99**
**Figure 4.5** ..... **100**
**Figure 4.6** ..... **101**

# Chapter 1

# Introduction

The heart responds to ever-present changes in environmental stimuli with an array of responses, including alterations in systolic contraction, diastolic relaxation, and heart rate. Beyond this, another critical component of the cardiac response to stress is robust change – either up or down – in cardiac mass[1]. The heart is capable of substantial increases and declines in mass, and those changes can take place in remarkably short periods of time.

Many of the environmental signals converging on the heart are physiological in nature, including postnatal growth, exercise, or pregnancy; here, cardiac mass increases or decreases rapidly and yet structure and function are preserved[2]. Many influences converging on the heart, however, are pathological, occurring in the context of disease. These include neurohormonal activation, hypertension, or myocardial injury, stressors that trigger perturbations in metabolic, structural, and functional properties of the heart. In the case of the former (physiological hypertrophy) untoward sequelae do not arise over time; in the case of the latter (pathological hypertrophy) progression to a state of ventricular wall thinning, systolic and diastolic dysfunction, and a clinical syndrome of heart failure is common[3]. Further, both pathological hypertrophy and heart failure are associated with markedly increased risk of malignant ventricular arrhythmia[4]. From a teleological perspective, the early phases of cardiac hypertrophy may be a compensatory response to increased workload, serving to normalize wall stress and thereby minimize oxygen consumption. In the long run,

however, pathological hypertrophy is a milestone in the pathogenesis of heart failure[4].

Unlike the physiological hypertrophic growth response, pathological hypertrophy entails more than just increases in myocyte size and heightened sarcomeric organization. Rather, a shift toward glycolytic metabolism, alterations in calcium storage and handling, changes in contractility, and reactivation of a fetal gene program are seen[1]. In this way, patterns of gene expression mimic those seen in early embryonic development. The myosin composition of the cardiomyocyte is altered, and extracellular deposition of collagen leads to fibrosis, together contributing, at least in part, to diminished contractile performance[5]. These distinguishing characteristics of pathological hypertrophy raise obvious questions regarding whether this response is adaptive and protective. Indeed, preclinical studies have shown that attenuation of load-induced hypertrophy is well tolerated and furthermore, ventricular dilation and decompensation do not occur[6]. Correlative studies in patients with heart disease similarly support this contention[7]. Thus, suppression of pathological cardiac hypertrophy per se may be a viable target for therapeutic intervention[8].

Autophagy, an ancient lysosome-mediated catabolism pathway, is an attractive mechanism for consideration as a means of controlling the hypertrophic response[9]. Autophagy, or more specifically, macroautophagy, is an evolutionarily conserved and ubiquitous mechanism for the degradation of long-lived proteins and the clearance of organelles[10]. While it may seem paradoxical to consider a

degradative mechanism in the context of cellular growth, hypertrophic remodeling of any cell, particularly a cell with the complex architecture of a myocyte, involves more than simple addition of new proteins; instead, dismantling and remodeling of existing cellular elements are required. Indeed, evidence for lysosomal pathway activation in heart disease has been reported for decades in both human heart failure and in animal models of disease[11], but it is only recently that this increase in activity has been tied to autophagy and its functional significance tested. Just as in understanding the hypertrophic process itself, a key to understanding the role(s) of autophagy in the heart involves elucidating its context-dependent adaptive versus maladaptive potential. One model holds that basal autophagic flux is fundamental to cellular homeostasis, but exuberant stress-induced activation of autophagy can be maladaptive.

## Basal Autophagy

The most potent physiological inducer of autophagy is nutrient depletion. Limitations in various nutrients, such as amino acids, glucose, growth factors, and oxygen each induce autophagy, with amino acid withdrawal provoking the greatest activation of autophagy in mammalian cells in culture. Autophagy is robustly induced in all tissues in the early neonatal period immediately after the abrupt interruption of the previously continuous supply of nutrients via the placenta and before the newborn has access to milk[12]. Indeed, the robust autophagic response at mammalian birth is necessary for survival, with neonatal

lethality observed in animals harboring mutations in essential autophagy genes[12, 13].

Autophagic flux is required for survival of neonatal rat cardiomyocytes (NRCMs) maintained in culture; short hairpin RNA (shRNA) targeting Atg7 reduces the number of viable cells as compared with nonspecific shRNA[14]. In an intact organ such as the heart, terminally differentiated cardiomyocytes are dependent on autophagy, not just for protection from starvation, but for protein quality control and removal of damaged organelles. Inactivation of Atg5 in the adult heart by tamoxifen-inducible Cre-Lox recombination leads to rapid left ventricular dilation and contractile dysfunction[14]. Atg5-inactivated cardiomyocytes exhibited disorganized sarcomere structure, misalignment and aggregation of mitochondria, and aberrant concentric membranous structures[14]. These results lend strong credence to the notion that constitutive cardiomyocyte autophagy is a critical housekeeping function which is fundamentally required for homeostasis under basal, resting conditions.

## Ischemia/Reperfusion Injury

Ischemic heart disease is enormously prevalent, exacting a huge toll on individuals and society. When exposed to ischemia, a given tissue is deprived of both nutrients and oxygen. In most clinically relevant instances, ischemia is followed by a reperfusion phase where arterial blood supply is restored either spontaneously or therapeutically. Reperfusion elicits a host of cellular responses, including activation of a number of signaling cascades, accumulation of reactive

oxygen species (ROS), and more[15, 16]. Thus, the biology of ischemia/reperfusion (I/R) injury is complex, as are the attendant autophagic responses.

As in the case of starvation, autophagy is activated during ischemia. And in additional analogy to starvation, ischemia-induced autophagy appears to be protective. One of the earliest studies demonstrating autophagosome formation in the heart employed an ex vivo rabbit heart model subjected to 40 minutes of ischemia[11]. Autophagosomes were detected containing numerous mitochondria suggesting that the activation of autophagy was serving to remove these damaged organelles. Lengthening the ischemic period to 60 minutes triggered the appearance of large and dysfunctional lysosomes, suggesting an impairment of autophagosome-lysosome fusion. Increased autophagy was correlated with functional recovery, but prolonged ischemia resulted in irreversible damage and contractile dysfunction. More recent studies in chronically ischemic swine myocardium confirmed these earlier findings of increased autophagy induction and lysosomal activity[17]. Furthermore, it was noted that areas of the heart with increased autophagy also exhibited fewer apoptotic cells, suggesting that the autophagic response protected against apoptotic cell death. At this point in time, the preponderance of evidence suggests that cardiomyocyte autophagy is protective during ischemia, possibly by providing an alternate energy source for cell survival.

Efforts to model cardiomyocyte I/R injury in vitro have yielded divergent evidence regarding whether autophagy is protective or maladaptive in this

context. When cardiomyocytes of the murine atrial cardiomyocyte-derived HL-1 cell line were exposed to 2 hours of ischemia and 5 hours of reperfusion, the formation of autophagosomes was inhibited in the ischemic phase and accumulation was not seen until reperfusion commenced[18]. The assays employed by these investigators relied upon accumulation of green fluorescent protein-tagged LC3 (GFP-LC3) puncta as markers of autophagosomes. Further, lysosomal inhibitors were used to suppress autophagic vacuole degradation in order to assess autophagic flux. Thus, these results were indicative of a block in autophagy induction during ischemia and dysfunctional degradation of autophagosomes during reperfusion. Pharmacological and genetic manipulations to increase autophagic flux were protective, possibly by blocking apoptosis. Conversely, further inhibiting autophagic flux led to greater cellular injury.

Glucose deprivation, a milder mimetic of myocardial ischemia and one more in line with starvation, induced autophagy in cultured cardiomyocytes, and pharmacological blockade provoked declines in cell survival[19]. These studies suggest that autophagy may serve primarily to maintain energy production during acute ischemia but evolves to accomplish clearance of damaged organelles during chronic ischemia or reperfusion.

Clearly, careful consideration must be given to the protocols employed to simulate I/R in vitro. In some instances, for example, it is likely that energy constraints imposed by an extensive ischemic protocol preclude autophagy activation. Indeed, in the context of the intact heart, cardiomyocytes likely

experience more nuanced I/R stress with different cells subjected to varying levels of nutrient and oxygen deprivation.

Studies in vivo similarly point to a dichotomous role for autophagy in I/R. Matsui et al. reported apparent increases in LC3-II accumulation, a surrogate for autophagic activity, with 20 minutes of ischemia followed by 20 minutes of reperfusion[19]. Importantly, it must be noted that measurements of steady-state LC3-II levels do not differentiate between induction of autophagy upstream of LC3-II (increased flux) versus a block in downstream vacuole degradation. Nevertheless, it was found that AMPK, an established cellular nutrient sensor, was activated transiently during ischemia and that this activity was required to induce autophagy. When mice haploinsufficient for Beclin 1 (Beclin 1+/-) were exposed to I/R, the autophagic response was attenuated, as was the extent of myocardial infarction and number of apoptotic cells, suggesting an overall maladaptive role for autophagy. In aggregate, these findings suggest that autophagic flux triggered by ischemia may be beneficial (analogous to starvation), whereas that elicited by reperfusion may be harmful.

The purported maladaptive second wave of autophagic activation upon reperfusion is an intriguing basis for probing the mechanism by which autophagy contributes to I/R injury. Increased expression of Beclin 1 accompanies the autophagic activity seen in an isolated rat heart model of I/R[20], and some evidence suggests that increased Beclin 1 expression can be indicative of maladaptive autophagic activity[19].

Another BH3 domain-containing protein up-regulated in I/R is Bnip3, a protein that has been linked with cell death[21]. Genetic ablation of Bnip3 was protective in I/R, partially rescuing declines in systolic performance and ventricular dilatation, interestingly, however, without affecting infarct size. Conversely, cardiomyocyte-specific over-expression of Bnip3 induced progressive ventricular dilation and impaired systolic performance, with increased markers of apoptosis. Expression of Bnip3 is driven by hypoxia-dependent factor-1 (Hif-1), and Bnip3 participates in the elimination of defective mitochondria in hypoxia[22]. Bnip3 provokes mitochondrial fragmentation and subsequent autophagy in cardiac myocytes, and suppression of Bnip3 using a dominant-negative mutant protects against I/R injury[23]. In aggregate, these studies point to a central – and intricate – role of cardiomyocyte autophagy in the maladaptive remodeling of I/R states.

## Hypertrophy and Failure

Hypertrophic growth is a prominent response of the heart to increases in afterload such as that which occurs with hypertension and valvular disease. The growth response involves increases in protein synthesis, remodeling of contractile elements, and formation of new sarcomeres. An established model for this process is surgical thoracic aortic constriction (TAC). Here, a carefully calibrated stenosis is imposed surgically on the aorta, prompting an immediate increase in afterload. Studied in this context, autophagy is rapidly induced as early as 24 hours after surgery, reaches peak levels at 48-72 hours and remains

elevated at 3 weeks[24]. In Beclin $1^{+/-}$ mice, where autophagic activity is attenuated approximately 50%, load-induced increases in autophagy were diminished and a modest protection from systolic dysfunction was observed. Conversely, in transgenic mice with cardiomyocyte restricted over-expression of Beclin 1, autophagic activity was markedly increased and the pathological response was amplified, with increases in hypertrophy and fibrosis, accelerated ventricular dilatation and declines in systolic performance, ultimately culminating in early mortality. These combined findings point to a maladaptive role for autophagy in the setting of severe pressure overload stress.

Inactivation of a different gene required for autophagy, Atg5, points to an adaptive role for autophagy[14]. Mice harboring a cardiomyocyte-specific deletion of Atg5 during cardiogenesis ($Atg5^{f/f}$;MLC2v-$Cre^{+}$) showed no cardiac hypertrophy or dysfunction well into adulthood. When subjected to TAC, however, the mice developed cardiac dysfunction and left ventricular dilation within 1 week. Interestingly, heart weight/body weight ratios and cardiomyocyte cross-sectional areas increased to a similar degree in mutants and controls subjected to TAC. Instead, polyubiquitinated proteins, endoplasmic reticulum (ER) stress, and markers of apoptosis were more highly induced in the autophagy-deficient mice. These results suggest that autophagy does not play a role in regulating the cardiomyocyte hypertrophy induced by pressure overload.

Here again, the dichotomous role for autophagy in a disease process is evident. Discounting trivial explanations such as differences in surgical technique,

these two studies provide an interesting basis for interpreting the role of autophagy in pressure-overload hypertrophy. The major difference between the studies lies in the mouse models used. Cardiac-specific inactivation of Atg5 results in complete abrogation of autophagy in cardiomyocytes, whereas Beclin $1^{+/-}$ mice have only diminished autophagic flux (≈50%). The $Atg5^{f/f}$;MLC2v-$Cre^{+}$ mice showed no cardiac phenotype prior to being stressed by TAC, suggestive of some sort of compensation for the complete loss of basal autophagy. Once exposed to the stress of pressure overload, however, this compensatory mechanism may have been overwhelmed and cardiomyocytes were unable to clear protein and cellular debris, leading to ER stress and perhaps apoptosis. Noting that the degree of hypertrophic growth in response to TAC was no greater in comparison to controls while systolic dysfunction was exaggerated, perhaps the explanation is that a stressed, autophagy-disabled cardiomyocyte is uniquely compromised in terms of contractile performance. In contrast, Beclin $1^{+/-}$ mice maintain basal levels of autophagic flux but yet stress-induced activation of autophagy is blunted; this may allow cardiomyocytes to maintain critical levels of contractility, but not enough reserve autophagy capacity to allow for hypertrophic growth. In the Beclin 1 transgenics, the extra capacity for autophagy was exploited for exaggerated growth and eventual systolic dysfunction in response to the stress of pressure-overload. Thus, these three models exist on a continuum of autophagic activity where too little or too much autophagy in response to stress is maladaptive, whereas a certain amount of constitutive autophagic activity is both adaptive and required for cell survival[25].

## Central Thesis

I favor a model where pathological stress on the heart elicits an autophagic response in cardiac myocytes that can become maladaptive, possibly by eliminating cellular constituents (e.g. mitochondria) indiscriminately. Another model, which is not mutually exclusive with the quantitative "goldilocks model" (not too much, not too little…but just right) holds that basal autophagic flux is qualitatively different from stress-activated autophagy. The former maintains a housekeeping function, which is critical for survival by eliminating misfolded proteins, protein aggregates, and dysfunctional mitochondria that might provoke autophagic cell death. Conversely, stress-activated autophagy might target specific cellular substrates, including some which are important for cell function (e.g. normally functioning mitochondria). Indeed, precedent exists in other cell types for autophagic mechanisms targeting specific substrates, as opposed to a random scavenging of the cell[26]. Either way, a case can be made for therapeutic manipulation of autophagy within a zone that is adaptive.

Successful therapeutic manipulation of cardiomyocyte autophagy for clinical benefit will depend on additional dissection of underlying mechanisms. Unveiling the qualitative or quantitative features that determine whether autophagy is adaptive or maladaptive will raise the prospect of enhancing the advantageous aspects while inhibiting the deleterious ones. To this end, in this thesis, I will:

1. Identify a signaling pathway that is essential for maladaptive autophagy necessary for pressure-overload induced hypertrophy.
2. Investigate skeletal muscle atrophy as a model for understanding anti-growth autophagy.
3. Investigate mitochondria as the target for maladaptive cardiomyocyte autophagy.

# Chapter 2

# RalGDS Dependent Cardiomyocyte Autophagy Is Necessary For Load-Induced Ventricular Hypertrophy

## Introduction

In response to pathological stress such as neurohormonal activation, hypertension, or myocardial injury, the heart is capable of a robust increase in cardiac mass[1]. From a teleological perspective, the early phases of cardiac hypertrophy may be a compensatory response to increased workload, serving to normalize wall stress and thereby minimize oxygen consumption. In the long run, however, pathological hypertrophy is a milestone in the pathogenesis of heart failure[4]. Numerous signaling pathways have been implicated in the regulation of cardiac hypertrophy[27]. More recently, autophagy has emerged as critical process involved in cardiac hypertrophy[25].

Autophagy, or more precisely, macroautophagy, is an evolutionarily conserved and ubiquitous mechanism for the degradation of long-lived proteins and clearance of organelles[28]. Autophagy is involved in numerous disease processes, including neurodegeneration, cancer, and infectious disease[29]. The Hill lab and others have demonstrated a role for autophagy in cardiac hypertrophy, as well. A major question that remains largely unanswered about autophagy in the heart, and disease in general, is whether autophagy is an adaptive or maladaptive response to stress. Our findings point to a maladaptive role for autophagy in the setting of severe pressure overload stress[24]. Conversely, inactivation of a different gene required for autophagy, Atg5, points to an adaptive role for autophagy[14]. These seemingly contradicting results may imply that autophagic activity lies on a continuum, where too little or too much

autophagy in response to stress is maladaptive, but a minimum amount of constitutive autophagic activity is both adaptive and required for cell survival.

The dichotomous roles of cardiac hypertrophy and cardiomyocyte autophagy led me to consider a common feature of the two processes: membrane biogenesis and processing. A plausible nexus for these two processes lies in the exocyst, an octomeric protein complex involved in vesicle trafficking. It serves a necessary role in the targeting of Golgi-derived vesicles to the basolateral membrane of polarized epithelial cells and to the growth cones of differentiating PC12 cells[30-32]. Recent work has demonstrated a role for the exocyst in autophagosome assembly as well. The small G protein, RalB, and an Exo84-dependent subcomplex of the exocyst were demonstrated to be critical for nutrient starvation and pathogen-induced autophagosome formation[33]. While many small GTPases have critical effects on cardiac plasticity[34], the role of small G protein-dependent membrane trafficking in stress-induced cardiomyocyte remodeling and autophagy remains largely unexplored.

Previous studies have suggested a role for the Ral family of small GTPases through its guanine exchange factor (GEF), Ral GDP dissociation stimulator (RalGDS), in cardiac hypertrophy. Cardiotrophin-1 (CT-1) activated RalGDS mRNA expression and induced Ral activation in an in vitro model of cardiac hypertrophy; similarly Ral activity was elevated in hypertrophied hearts in a rat aortic banding model[35]. Moving forward, the exact mechanism of RalGDS influence on cardiac hypertrophy requires clarification. Here, I set out to test the

role of small G protein-dependent membrane trafficking via RalGDS/Ral signaling in stress-induced cardiomyocyte remodeling and autophagy.

## Materials & Methods

### Animal models and echocardiography

Male C57/BL6 mice (6–8 weeks old) were subjected to thoracic aortic constriction (TAC) for 3 weeks as previously described[6, 36]. Control animals underwent sham operations. The Animal Care and Use Committee of the University of Texas Southwestern Medical Center at Dallas approved all animal care and procedures. Echocardiograms were performed on conscious, gently restrained mice using a Vevo 2100 system with a MS400C scanhead. LVEDD and LVESD were measured from M-mode recordings. FS was calculated as (LVEDD - LVESD)/LVEDD and expressed as a percentage. All measurements were made at the level of the papillary muscles.

### Primary culture of neonatal cardiomyocytes, siRNA transfection and adenovirus infection

Neonatal rat cardiomyocytes were isolated and cultured as described previously[37]. After 24 hours, NRCMs were transfected with siRNA constructs (Ambion) using Lipofectamine RNAiMax (Invtirogen) in Optimem (Gibco) for 4 hours, and then switched to basal media: DMEM supplemented with 3% fetal bovine serum (FBS), BrdU, and antibiotics. After 48 hours, cells were infected

with adenovirus (MOI 10) for 1 hour in Optimem and then switched to basal media.

## Real-time RT-PCR

Total RNA was harvested from NRVMs or mouse LV using TRIzol (Invitrogen) according to the manufacturer's protocol. cDNA was prepared from RNA using a high capacity cDNA reverse transcription kit (Applied Biosystems). Real-time PCR was performed using SYBR green on an ABI 7000 Prism Sequence Detection System (Applied Biosystems). To confirm amplification specificity, the PCR products were subjected to melting curve analysis. Negative controls containing water instead of cDNA were run concomitantly. Data for each transcript were normalized to reactions performed using GAPDH or 18S rRNA primers, and fold change was determined using the comparative threshold method[38].

## Immunoblot analysis

Tissues were either homogenized immediately or quick frozen in liquid nitrogen and stored at −80 °C for later use. To harvest protein, tissues were homogenized at 4°C in M-PER® mammalian protein extraction reagent (Thermo Scientific), with added protease inhibitors (Roche) and phosphatase inhibitors (Sigma). Whole cell lysates from cultured neonatal myocytes were prepared by directly harvesting cells in M-PER® mammalian protein extraction reagent (Thermo Scientific). Homogenates were passed over glass wool to remove DNA. Proteins were separated by SDS/PAGE, transferred to a supported nitrocellulose

membrane, and immunoblotted. All antibodies were purchased from Cell Signaling Technology, except α-tubulin (Sigma-Aldrich) and GAPDH (Santa Cruz Biotechnology). Blots were scanned, and bands were quantified using Odyssey Licor (version 3.0) imaging system.

## Histology

All tissues were fixed in 4% paraformaldehyde and were transferred to PBS followed by paraffin embedding.

## Myocyte Cross-sectional Area

Images of tissues stained with wheat germ agglutinin were paraffin fixed (Vector Laboratories), and images were acquired on a confocal microscope (TCS SP5; Leica) with Leica LAS AF software. The following lenses were used: HC PL APO 20×/0.70, HCX PL APO 40×/1.25-0.75 oil, and HCX PL APO 63×/1.40-0.60 oil. All images were taken at room temperature and processed in ImageJ for CSA analysis. Occasionally, images were linearly rescaled to optimize brightness and contrast uniformly without altering, masking, or eliminating data. CSA was calculated from at least 15 cells per condition and from representative triplicate experiments.

## Statistics

Data are presented as mean ± SD or SEM. The unpaired Student's t test was used for comparison between two groups, and ANOVA with Bonferroni

correction was used for comparison among multiple groups. Values of $p < 0.05$ were considered significant.

## Results

### RalB is necessary for cardiomyocyte autophagy

To test whether Ral small GTPases are required for cardiomyocyte autophagy, I knocked down the RalA or RalB isoforms in neonatal rat cardiomyocytes (NRCMs). The siRNA constructs were specific for their respective isoform and were able to knock down their target 48 hours after transfection (Fig. 2.1 A). The most potent inducer of autophagy is starvation[28], so I simulated starvation by incubating NRCMs in Earle's Balanced Salt Solution (EBSS) for 2 hours (Fig. 2.1 C). Starvation led to increased levels of the faster migrating, lipidated form LC3-II, indicating an accumulation of autophagosomes. Concomitant treatment with the lysosomal inhibitor Bafilomycin A1 led to a further increase in LC3-II, demonstrating that the increase in LC3-II seen with starvation is indeed an induction of autophagic flux and not simply a block in degradation of autophagosomes. When expression of RalB was knocked down in NRCMs, the expected increase of LC3-II in response to starvation was lost. The NRCMs lacking RalA expression however, continued to manifest increased LC3-II when starved. Degradation of the autophagy substrate p62 was observed in response to starvation in NRCMs, as well. After knockdown of RalB, this degradation was attenuated. In fact, treatment with the lysosomal inhibitor failed to increase p62 in these cardiomyocytes, suggesting that p62 may be degraded by other

mechanisms. These results suggest that RalB is necessary for cardiomyocyte autophagy in response to starvation.

The autophagy response to starvation, and more specifically amino-acid withdrawal, is mediated by the release of mTOR-dependent inhibition[39]. To test whether knockdown of RalB was affecting autophagy induction by interfering with this pathway, I examined phosphorylation of mTOR and its substrate ribosomal protein s6. NRCMs exposed to EBSS showed diminished phosphorylation at serine 2448 of mTOR and marked loss of phosphorylation of s6 as well (Fig. 2.1 B). This response was similar when either RalA or RalB were knocked down, demonstrating that autophagy inhibition seen with loss of RalB was not due to a block in the mTOR response to starvation.

As an alternative method for inducing autophagy, I turned to pharmacological blockade of mTOR using the inhibitor Torin1[40]. Similar to starvation, direct mTOR inhibition by treatment with Torin1 for 2 hours led to increased LC3-II and degradation of p62 (Fig. 2.1 D). With lysosomal inhibition, LC3-II was further increased and p62 degradation blocked, demonstrating an induction of autophagy flux by Torin1. In NRCMs lacking RalB however, autophagy flux was lost as indicated by a failure to increase LC3-II and a muted degradation of p62 (Fig. 2.1 D). These results suggest that RalB is necessary for cardiomyocyte autophagy induced by pharmacological blockade of mTOR.

As yet another method for testing autophagy, I evaluated adenoviral-mediated expression of GFP-tagged LC3 in NRCM's (Fig. 2.1 E). Exposure to

EBSS and Torin1 for 2 hours induced localization of GFP-LC3 to distinct puncta, indicative of autophagosome accumulation. The numbers of GFP-positive puncta per cell were significantly elevated in NRCMs in response to EBSS and Torin1 (Fig. 2.1 F). NRCMs lacking RalB did not show an increase in GFP positive puncta in response to either treatment (Fig. 2.1 F). These results provide additional evidence that the RalB isoform is necessary for cardiomyocyte autophagy.

## RalGDS is necessary for autophagy

Next, I asked whether the guanine-exchange factor (GEF) for the Ral family GTPases, RalGDS, was necessary for autophagy. I utilized mouse embryonic fibroblasts (MEFs) that were homozygous deleted (KO), heterozygous deleted (HET), or wild type (WT) for the RalGDS allele. Autophagic flux in response to starvation was intact in the WT and HET MEFs as indicated by accumulating LC3-II when treated with EBSS and the lysosomal inhibitor for 2 hours (Fig. 2.2 A). In the KO MEFs, however, LC3-II accumulation was abolished and blunted under basal or starvation conditions, respectively. Degradation of p62 followed a similar pattern of autophagic flux in the MEFs. In WT and HET cells, the abundance of p62 diminished upon starvation, but in the KO MEFs, p62 protein accumulated in response to starvation. Taken together, these results implicate RalGDS as a GEF necessary for starvation-induced autophagy.

I tested further the necessity of RalGDS for cardiomyocyte autophagy in response to pharmacological blockade of mTOR. I treated MEFs for 2 hours with

Torin1 and Bafilomycin A1. The WT and HET MEFs were competent for autophagic flux, demonstrating an increase in LC3-II accumulation in response to this treatment, while KO MEFs failed to do so (Fig. 2.2 B). Additionally, degradation of p62 upon Torin1 treatment was lost in the KO MEFs. These results led me to conclude that RalGDS is necessary for autophagy.

I next tested whether RalGDS was necessary for cardiomyocyte autophagy. I knocked down RalGDS using two independent siRNA oligos in NRCMs and treated with 2 hours of starvation or pharmacological blockade of mTOR, with or without lysosomal inhibition. As expected cells, NRCMs treated with control siRNA were competent for autophagic flux, responding to 2 hours of starvation and Torin1 treatment with an increase in LC3-II accumulation and a further increase when Bafilomycin A1 was added (Fig. 2.2 C & D). NRCMs treated with siRNA for RalGDS on the other hand exhibited blunted autophagic flux. Only modest increases in LC3-II accumulation were demonstrated when the NRCMs were additionally challenged with lysosomal inhibition (Fig. 2.2 C & D).

Additionally, I also employed the GFP-LC3 punctae formation assay in NRCMs knocked down for RalGDS. As compared to the NRCMs treated with control siRNA, those treated with siRNA for RalGDS showed a significantly diminished number of GFP-LC3 punctae in response to both starvation and Torin1 treatment of 2 hours (Fig. 2.2 E & F). These results combined demonstrate that RalGDS is necessary for cardiomyocyte autophagy.

## RalGDS$^{-/-}$ hearts manifested a blunted growth response and preserved function in response to pressure-overload stress

Having established the necessity for RalGDS in cardiomyocyte autophagy, I wanted to examine further the role of RalGDS-dependent cardiomyocyte autophagy in pathological cardiac remodeling. I used a model of moderate pressure overload induced by transverse aortic constriction (TAC). In our hands, this model induces cardiac hypertrophic growth that reaches steady state at 3 weeks and does not manifest clinical heart failure at that time point[6]. Male mice lacking RalGDS (KO) and their wild-type (WT) littermates, aged 8 to 10 weeks, were subjected to pressure overload stress by thoracic aortic constriction (TAC) or sham operation. After 3 weeks, hearts from KO mice manifested a blunted growth response (Fig. 2.3 A). The blunted growth response was quantified and normalized by (Fig. 2.3 B) heart weight to body weight ratios (HW/BW; WT, sham: 4.99 ± 0.53 mg/g, n=12; TAC: 6.90 ± 1.18, n=15; KO sham: 4.67 ± 0.49, n=11, TAC: 5.61 ± 0.55, n=12; $p<0.05$) and (Fig. 2.3 C) and heart weight to tibia length ratios (HW/TL; WT, sham: 8.52 ± 1.27 mg/mm, n=12; TAC: 11.44 ± 1.53, n=15; KO sham: 7.95 ± 0.84, n=11, TAC: 9.15 ± 0.96, n=12; $p<0.05$).

To assess cardiac function, echocardiograms were performed 3 weeks following surgery (Fig. 2.4 A). Fractional shortening was decreased mildly, yet significantly, in the WT mice (Fig. 2.4 B), while remaining essentially unchanged in the KO group (FS %; WT, sham: 70.9 ± 5.4 %, n=3; TAC: 53.2 ± 7.8, n=5; KO sham: 65.0 ± 13.1, n=7, TAC: 61.1 ± 9.2, n=6; $p<0.05$). These functional

differences were due to significant increases in WT mice in both left ventricular internal diameter in diastole (LVIDd; WT, sham: 2.8 ± 0.20 mm, n=3; TAC: 3.4 ± 0.53, n=5; KO sham: 3.1 ± 0.75, n=7, TAC: 3.1 ± 0.38, n=7; $p<0.05$; Fig. 2.4 C) and left ventricular internal diameter in systole (LVIDs; WT, sham: 0.81 ± 0.21 mm, n=3; TAC: 1.6 ± 0.52, n=5; KO sham: 1.2 ± 0.67, n=7, TAC: 1.2 ± 0.43, n=6, $p<0.05$; Fig. 2.4 D). Overall, the KO mice were protected from the slight drop in cardiac function in response to TAC seen in the WT.

Furthermore, the morphological and functional changes observed were matched at the cellular level. Staining with wheat germ agglutinin of transverse sections of ventricular septa allowed me to assess the size of cardiomyocytes (Fig. 2.5 A). I quantified the mean cross-sectional area of 80-100 cardiomyocytes in the ventricular septum from each of 3 mice per group (Fig. 2.5 B). While cardiomyocytes from WT mice were enlarged in response to TAC surgery, the cross-sectional area of cardiomyocytes from KO mice were not significantly increased (CSA; WT, sham: 505 ± 20 μm2; TAC: 733 ± 27; KO sham: 484 ± 14, TAC: 557 ± 15; $p<0.05$). Interestingly, TAC-induced activation of the fetal gene program was similar in both genotypes despite the relative lack of hypertrophic growth in mutant hearts (Fig. 2.5 C).

## RalGDS$^{-/-}$ mice exhibit diminished load-induced and starvation-induced cardiomyocyte autophagy

Hearts from KO mice exhibit diminished load-induced cardiomyocyte autophagy in response to 3 weeks of pressure-overload stress. Heart lysates of

WT mice manifested increased LC3-II abundance with TAC surgery, whereas LC3-II accumulation is absent in hearts of KO mice (Fig. 2.6 A). Consistent with the TAC findings, KO mice manifested a blunted autophagic response to 24-hour fasting, suggesting a generalized defect in autophagy. Heart lysates of WT mice showed decreased LC3-I abundance during starvation, whereas LC3-I abundance remains elevated in KO mice (Fig. 2.6 D). Together, these data demonstrate a defect in autophagic flux in load-stressed KO heart in concert with blunted hypertrophic growth, consistent with prior findings that demonstrate a requirement of cardiomyocyte autophagic flux in cardiomyocyte hypertrophy[24].

## Discussion

### RalGDS is an activator of cardiomyocyte autophagy

My findings confirm that the small GTPase RalB is a necessary regulatory switch to promote autophagosomes biogenesis. Previous studies had shown that RalB and an Exo84-dependent subcomplex of the exocyst are critical for nutrient starvation and pathogen-induced autophagosome formation in human epithelial cells[33]. I have shown that RalB is also necessary for nutrient starvation induced autophagy in cardiomyocytes. Additionally, I demonstrated that RalB is indeed required proximal to autophagosomes biogenesis. Here I have shown that NRCMs lacking RalB are still able to sense nutrient depletion in terms of mTOR inhibition, but are unable to mount the necessary autophagy response.

RalA has recently been shown to promote mTORC1 activation, potentially through PLD1 and phosphatidic acid-dependent mTORC1/2 assembly[41-43]. I observed that when RalA is knocked down, autophagic flux at basal levels and in response to starvation is actually increased in comparison to control NRCMs. This implies a model where RalA and RalB represent an antagonistic switch for the autophagy response.

I have further demonstrated that RalGDS, a GEF for the Ral family of small GTPases, is itself a bona fide regulator necessary for cardiomyocyte autophagy. My results suggest that RalGDS is also a proximal regulator of autophagosome biogenesis, as mTOR inhibition in response to starvation is intact despite loss of RalGDS. Presumably, RalGDS functions as a GEF for RalB in its autophagy-activating role, but further studies are needed to confirm this model.

## RalGDS is necessary for cardiac hypertrophy in response to pressure-overload stress

My findings demonstrate that RalGDS is a critical regulator of cardiac hypertrophy. Previous findings had shown that overexpression of RalGDS in NRCMs was sufficient to activate the promoters of two fetal genes, beta myosin heavy chain and alpha skeletal muscle actin[35]. Here I have extended the role of RalGDS to an in vivo model of cardiac hypertrophy in response to pressure-overload stress. The hearts of mice lacking RalGDS manifested a blunted hypertrophic response in terms of gross tissue weight and myocyte size.

## Cardiomyocyte autophagy is required for load-induced hypertrophy

In preclinical studies[6] and correlative studies in patients with heart disease[7], attenuation of load-induced hypertrophy is well tolerated and furthermore, ventricular dilation and decompensation do not occur. I have shown here that in the RalGDS$^{-/-}$ hearts that manifest a blunted hypertrophic response, also maintain cardiac function in response to hemodynamic stress.

The hearts of mice lacking RalGDS failed to induce autophagy in response to pressure-overload. Presumably, RalGDS activation of autophagy is necessary for cardiac hypertrophy, but of course, further studies are needed to support this mechanism. My studies do however demonstrate that the exuberant stress-induced activation of autophagy can be maladaptive and that blocking the RalGDS/RalB induction of autophagy is a viable target for blocking this response.

## Figures

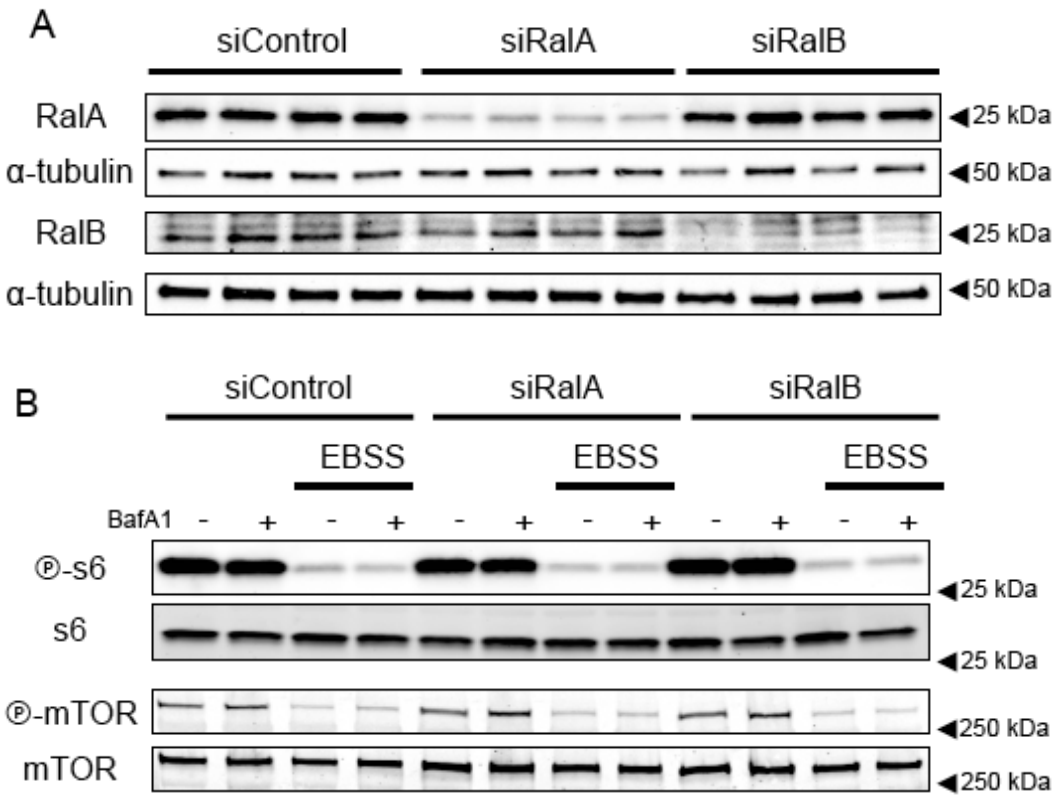


**Figure 2.1. RalB is necessary for autophagy.** Immunoblot detection of neonatal rat cardiomyocytes (NRCM) after 48 hour of siRNA mediated knockdown (**A**), and 2 hour starvation in Earle's Balanced Salt Solution (EBSS) (**B**) with or without Bafilomycin A1.

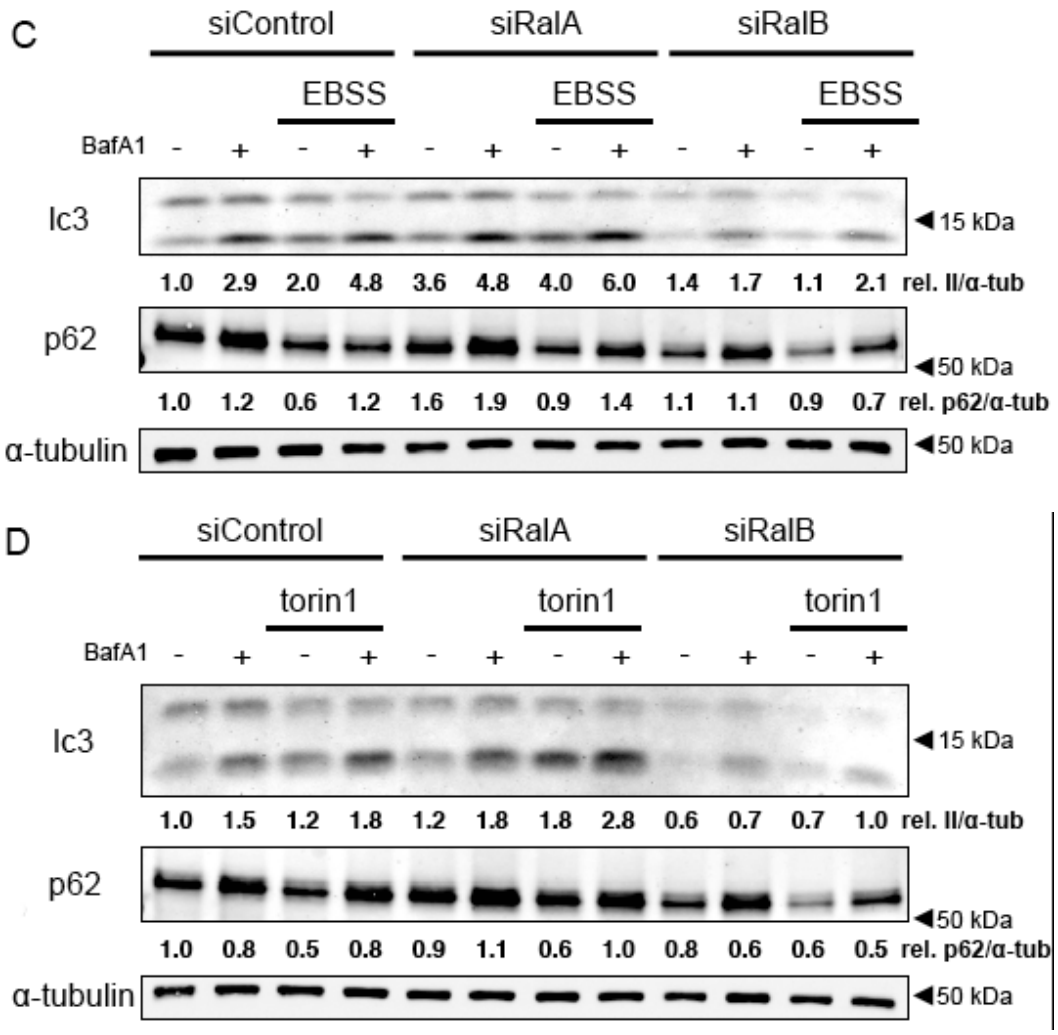


**Figure 2.1 continued.** Immunoblot detection of neonatal rat cardiomyocytes (NRCM) after 48 hour of siRNA mediated knockdown and 2 hour starvation in Earle's Balanced Salt Solution (EBSS) (**C**), or 2 hours treatment with Torin1 (**D**), with or without Bafilomycin A1.

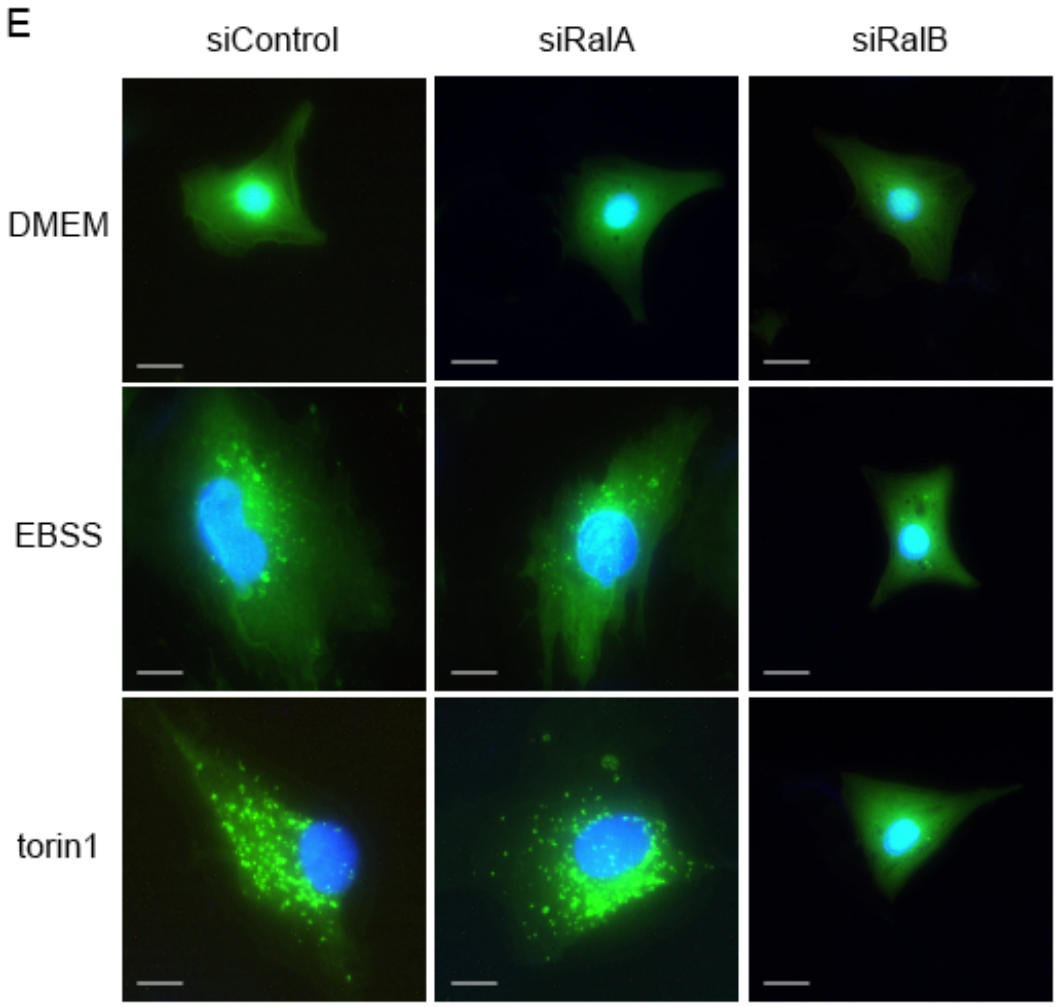


**Figure 2.1 continued.** (**E**) Representative images of cardiomyocytes expressing gfp-lc3 and exposed to EBSS or Torin1 for 2 hours.

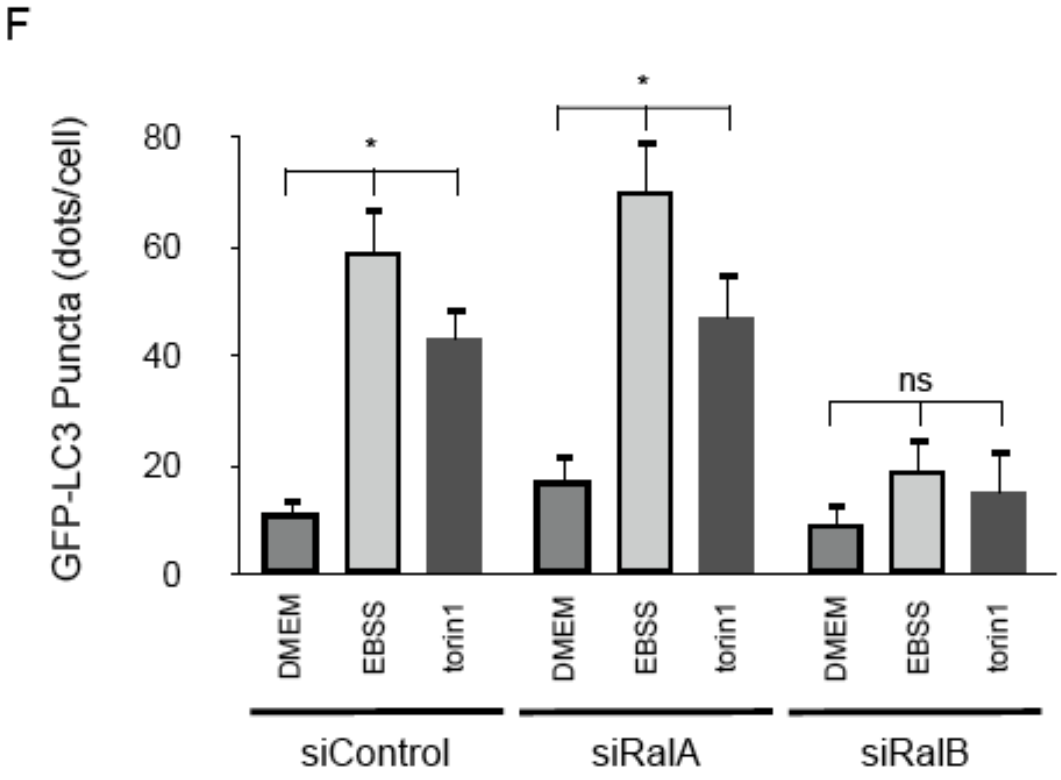


**Figure 2.1 continued.** (**F**) Quantification of gfp-lc3 puncta in 80 cells per treatment of cardiomyocytes expressing gfp-lc3 and exposed to EBSS or Torin1 for 2 hours.

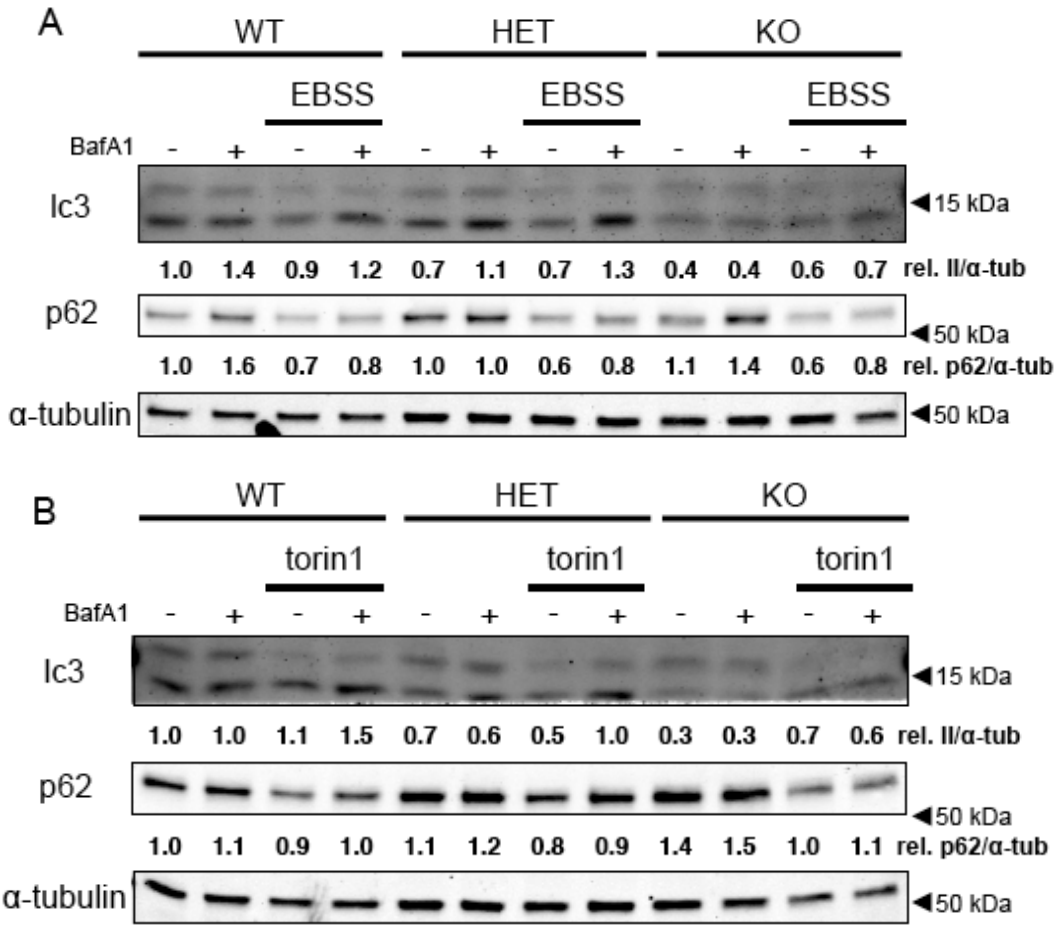


**Figure 2.2. RalGDS is necessary for autophagy.** Immunoblot detection of mouse embryonic fibroblast lysates of indicated genotype treated with 2 hours of treatment in (**A**) Earle's Balanced Salt Solution (EBSS) or (**B**) Torin1, and with or without Bafilomycin A1.

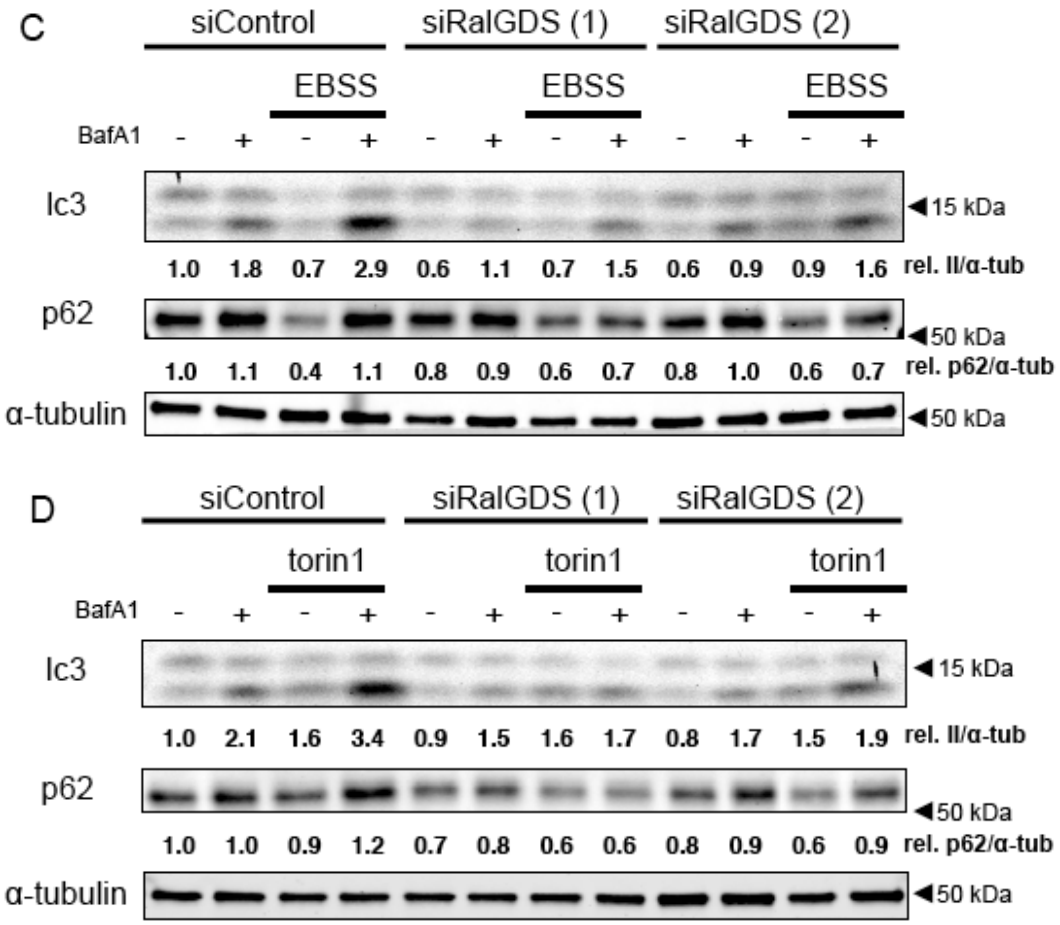


**Figure 2.2 continued.** Immnunoblot detection of neonatal rat cardiomyocyte (NRCM) lysates after 48 hour of siRNA mediated knockdown and 2 hours treatment in (**C**) Earle's Balanced Salt Solution (EBSS), or (**D**) Torin1, and with or without Bafilomycin A1.

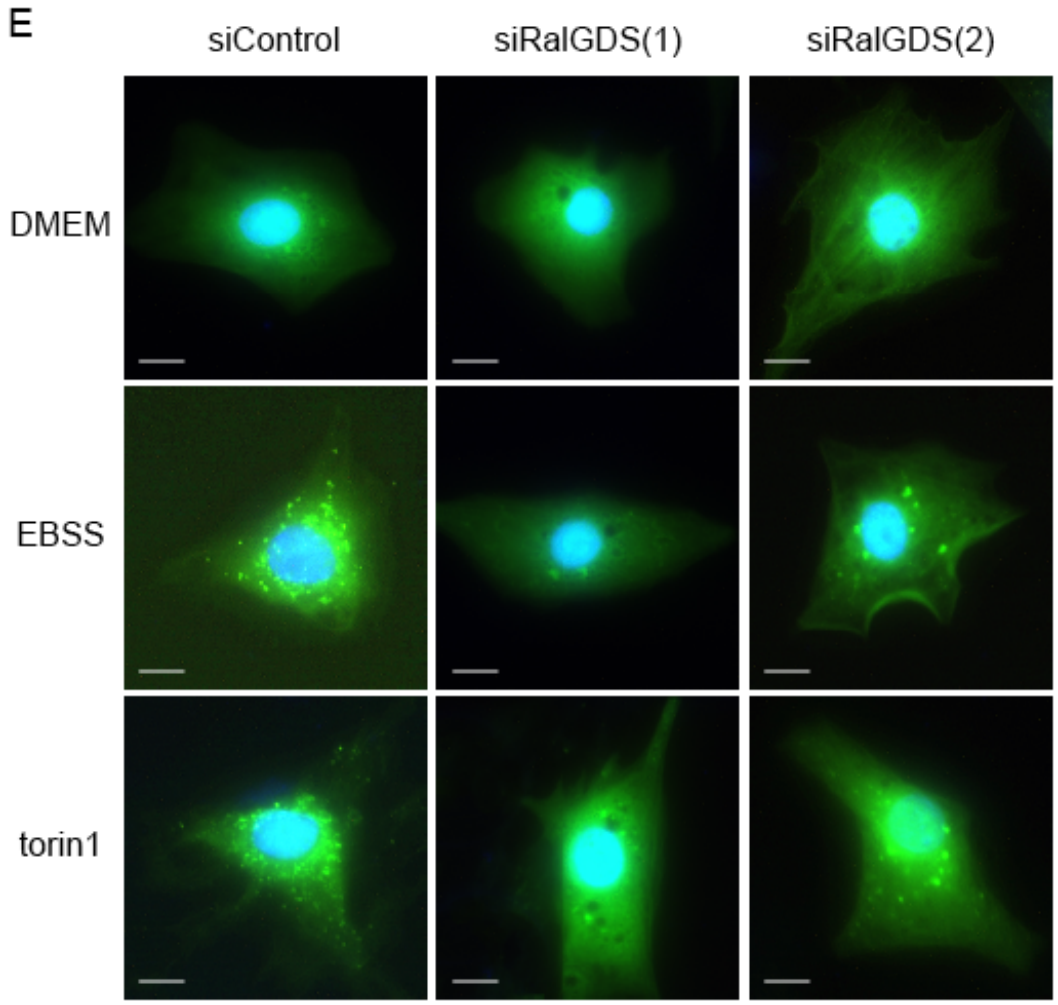


**Figure 2.2 continued.** (**E**) Representative images of cardiomyocytes expressing gfp-lc3 and exposed to EBSS or Torin1 for 2 hours.

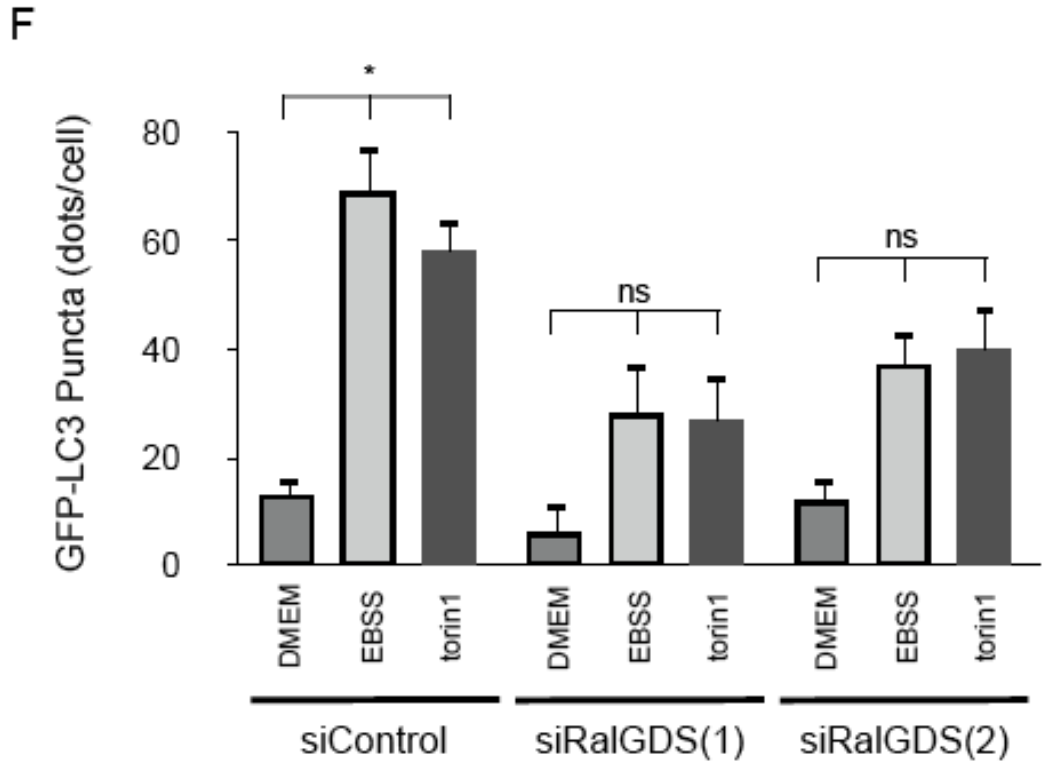


**Figure 2.2 continued.** (**F**) Quantification of gfp-lc3 puncta in 80 cells per treatment of cardiomyocytes expressing gfp-lc3 and exposed to EBSS or Torin1 for 2 hours.

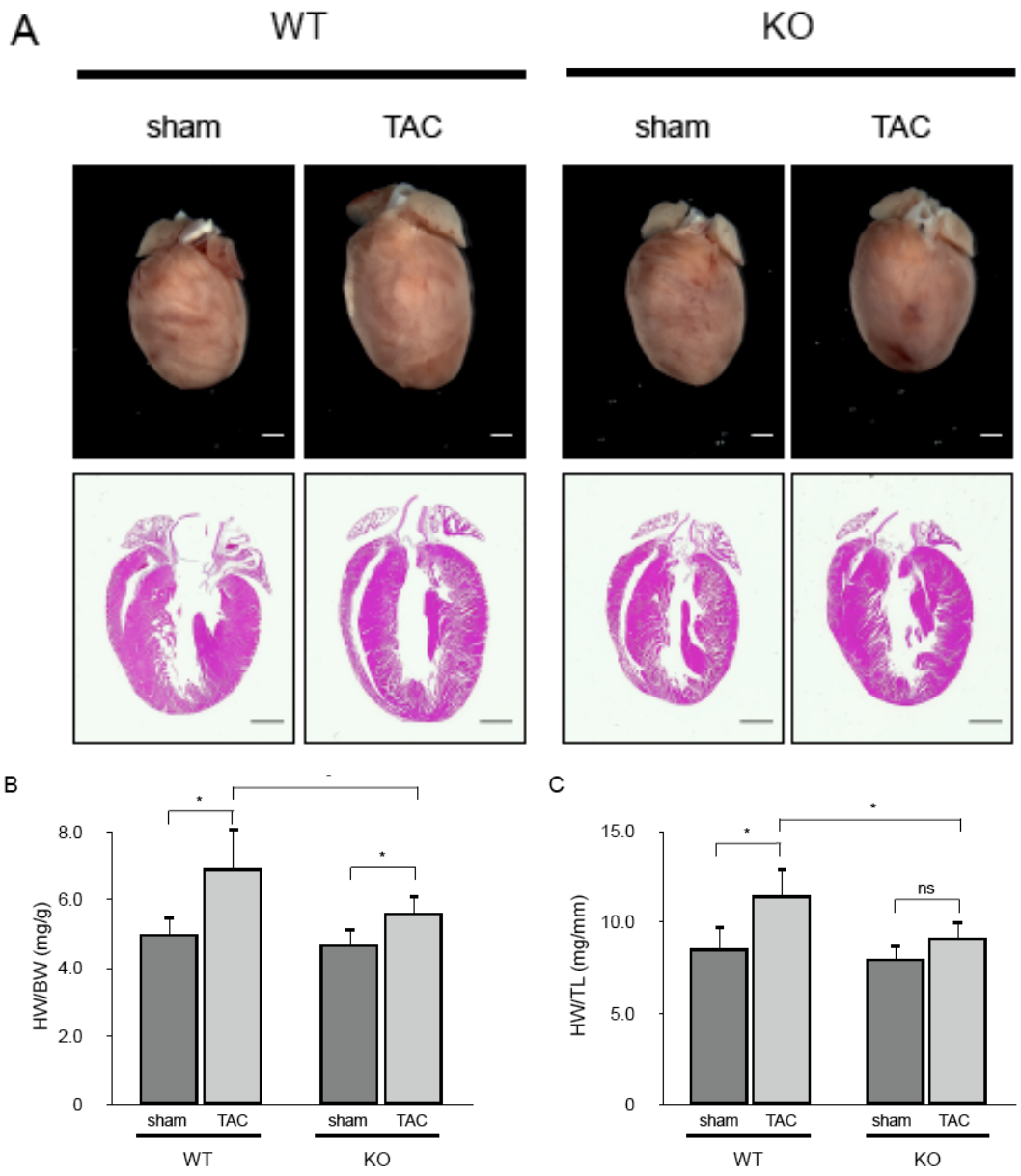


**Figure 2.3. RalGDS$^{-/-}$ hearts manifest a blunted growth response to pressure-overload stress.** Male mice lacking RalGDS (*Ralgds*$^{-/-}$) and their wild-type (WT) littermates, aged 8 to 10 weeks, were subjected to pressure overload stress by thoracic aortic constriction (TAC) or sham operation. After 3 weeks, hearts from *Ralgds*$^{-/-}$ mice manifested a blunted growth response as seen by representative (**A**) formalin-fixed whole hearts and H&E histology sections. The blunted growth response was quantified and normalized by (**B**) heart weight to body weight ratios and (**C**) heart weight to tibia length ratios.

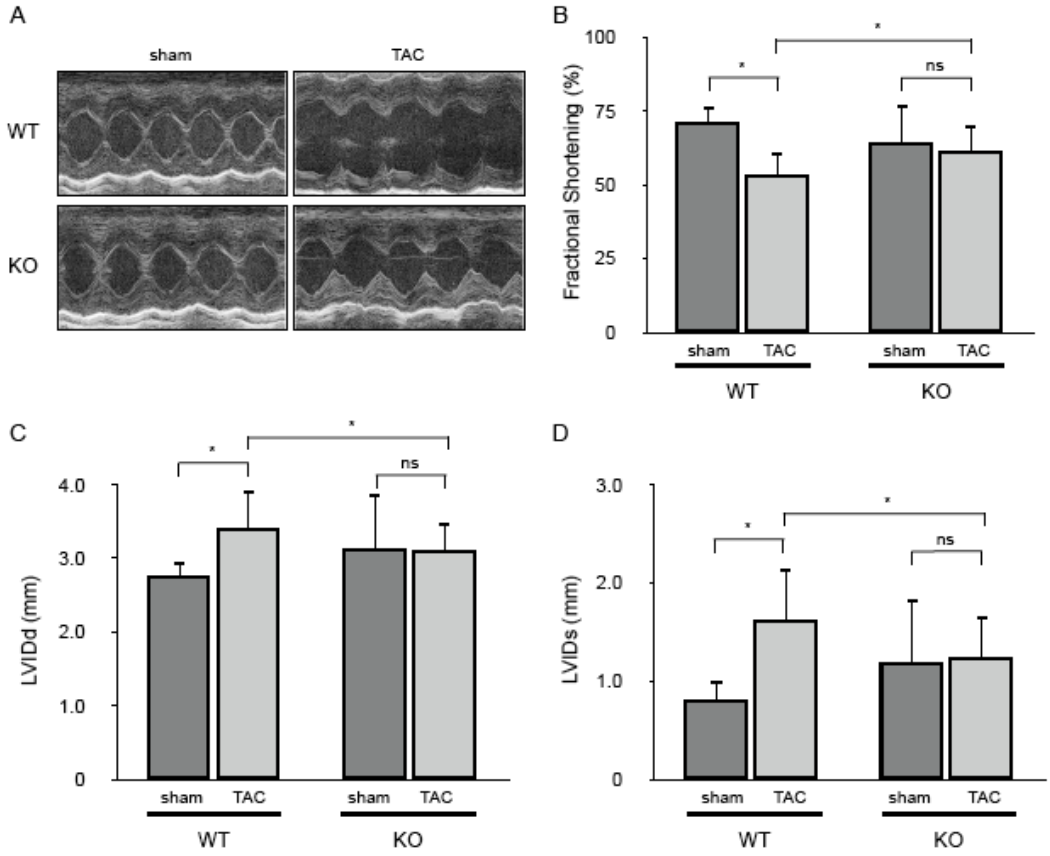


**Figure 2.4. RalGDS$^{-/-}$ hearts exhibit preserved function in response to pressure-overload stress.** (**A**) Representative M-mode tracings. (**B**) Fractional shortening (**C**) Left ventricular internal diameter in diastole (mm). (**D**) Left ventricular internal diameter in systole (mm).

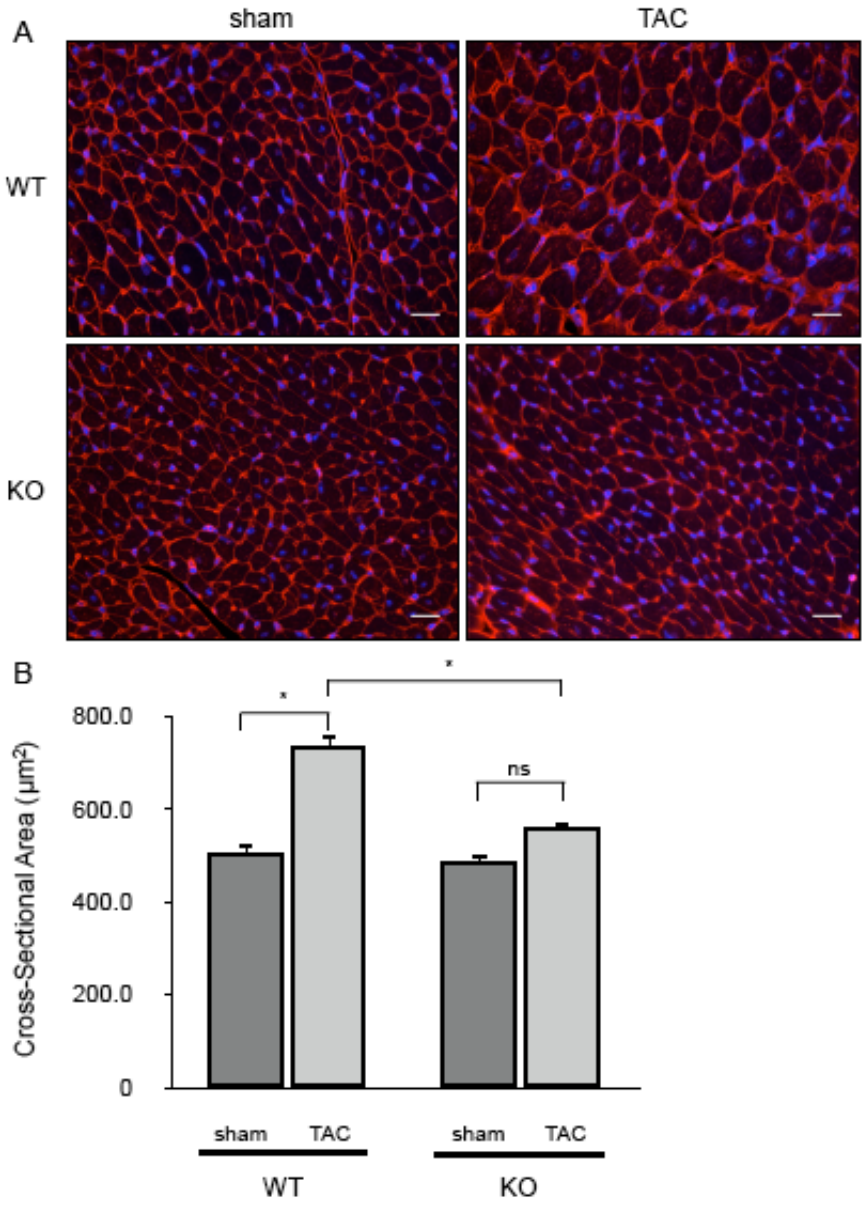


**Figure 2.5. Blunted growth response of RalGDS$^{-/-}$ hearts extends to cardiomyocyte size** (**A**) Representative sections of DAPI-labeled (blue) and wheat germ agglutinin stained (red) hearts. (**B**) Quantification of mean cross-sectional area of 80-100 cardiomyocytes in the ventricular septum from each of 3 mice per group.

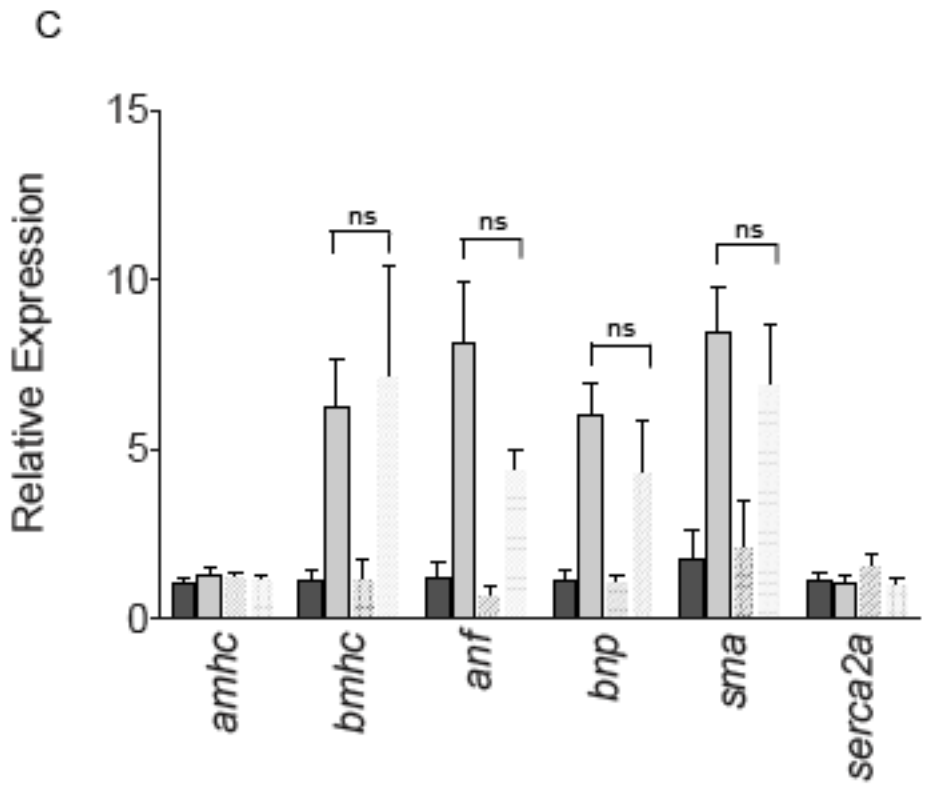


**Figure 2.5 continued.** (**C**) Mean relative mRNA expression in relation to 18s rRNA and normalized to sham +/+ levels (*amhc* alpha myosin heavy chain, *bmhc* beta myosin heavy chain, *anf* atrial natriuretic factor, *bnp* brain natriuretic peptide, *sma* smooth muscle actin, *serca2a* sarcoplasmic reticulum Ca(2+) ATPase).

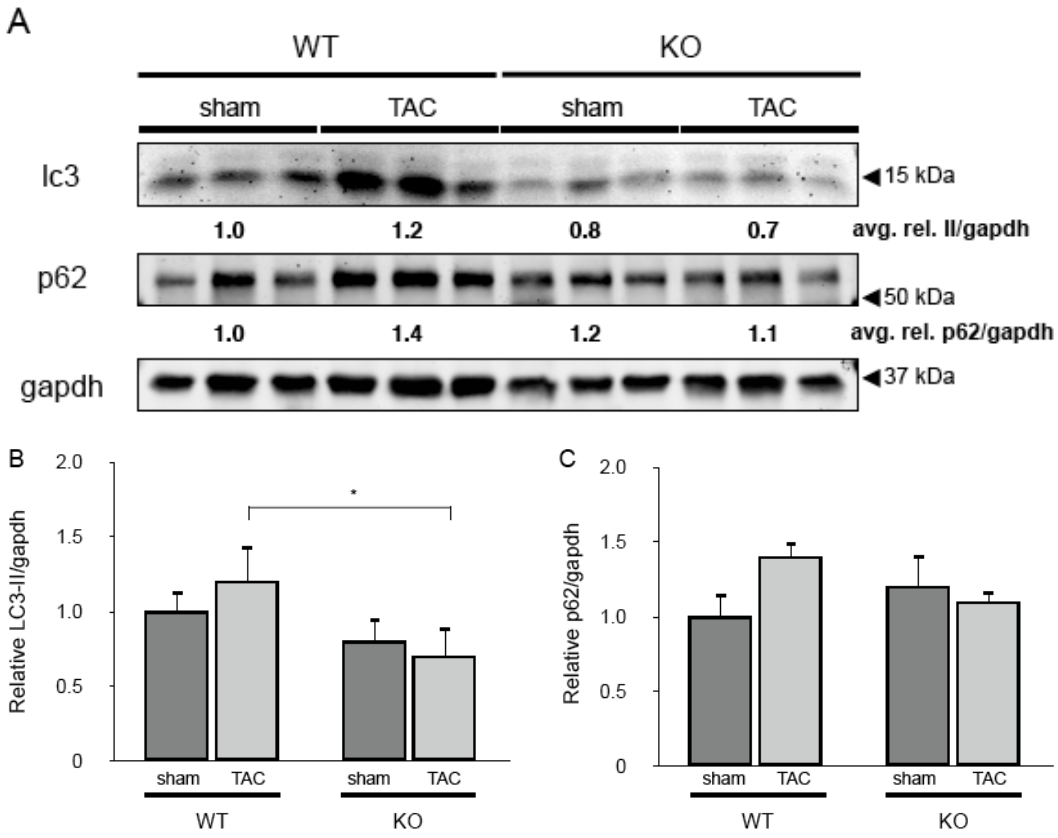


**Figure 2.6. RalGDS$^{-/-}$ mice exhibit diminished load-induced cardiomyocyte autophagy.** (**A**) Immunoblot detection of left-ventricle lysates following one week of TAC or sham surgery. Quantification of relative levels of (**B**) LC3 and (**C**) p62 expressed as fold induction over sham surgery of WT.

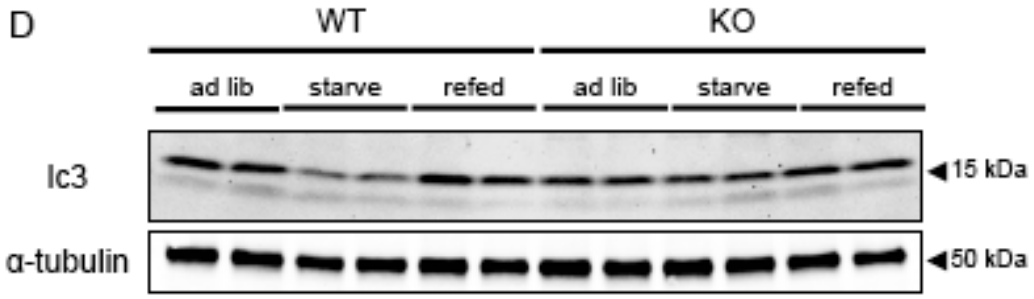


**Figure 2.6 continued.** (**D**) Immunoblot detection of left-ventricle lysates from mice fed *ad libidum* (ad lib), following 24 hours starvation (starve), or 24 hours starvation and 2 hours refeeding (refed).

# Chapter 3

# Foxo3a Controls Skeletal Muscle Atrophy

## Introduction

The heart is a remarkably plastic organ that responds to stimuli by growing or shrinking. These responses entail a delicate balance between numerous growth and degradation pathways wherein both types are active and inactive simultaneously, but to varying degrees. For example, we can think of a hypertrophied heart as one with more pro-growth pathways active than inactive and more pro-degradation pathways inactive than active. In this manner, it becomes apparent that to understand and target cardiac hypertrophy, we must not only study pro-growth pathways but also anti-growth and degradation mechanisms.

The serine-, threonine-phosphatase calcineurin is a well-characterized regulator of pro-growth pathways of cardiac hypertrophy. Binding of calmodulin in the presence of $Ca^{2+}$ relieves auto-inhibition, and calcineurin activates transcription of hypertrophic genes by dephosphorylating members of the nuclear factor of activated T-cell (NFAT) family of transcription factors[44]. Transgenic mice that express activated forms of calcineurin specifically in the heart develop cardiac hypertrophy and heart failure[45]. Conversely, knockout mice lacking a catalytic subunit of calcinuerin are resistant to pressure overload and pharmacologic induction of cardiac hypertrophy[46]. Blocking calcineurin activity, either pharmacologically[6] or genetically by overexpression of an endogenous inhibitor[47, 48], is also sufficient to attenuate cardiac hypertrophy. Calcinuerin is an

essential regulator of cardiac hypertrophy in response to pathological stimuli such as neurohormonal activation and chronic hemodynamic overload[27].

Physiological cardiac hypertrophy, such as post-natal growth or in response to exercise, is not associated with the untoward sequalae of pathlogical hypertrophy[49] and is governed by the phosphatidylinositol-3 kinase-dependent, serine-, threonine-kinase Akt pathway[50]. Genetic ablation of *Akt1* results in blunting of exercise-induced physiological hypertrophy and contractile function is impaired[51]. Interestingly, these mice responded to pressure overload with enhanced cardiac growth and diminished contractility, suggesting that the Akt pathway may function as both a positive regulator of physiological hypertrophy and negative regulator of pathological hypertrophy. Furthermore, cardiac-specific overexpression of a constitutively active form of Akt1 results in mild hypertrophy and preserved function, without pathological changes[52]. Using a cardiac-specific inducible Akt1 transgenic approach, another group found that mice develop physiological hypertrophy following short-term induction but pathological hypertrophy with longer periods of transgene induction[53]. Thus, the delineation between physiological and pathological hypertrophy may not be as distinct.

Downstream of Akt are the O subfamily of Forkhead/winged helix transcription factors (FoxO). Akt represses FoxO transcriptional activity by phosphorylating specific residues, leading to nuclear export and subsequent degradation of FoxO[54]. Phosphorylation of the FoxO3a isoform is increased in the heart in response to pressure overload, insulin, or Akt overexpression[55]. The

transcriptional target genes of FoxO include the "atrogenes" *Atrogin-1* (*Atg1*) and *MuRF1*[56, 57]. These ubiquitin ligases promote proteasomal activity and protein degradation. Thus, Akt exerts its hypertrophic effect partially by blocking FoxO-dependent degradation pathways. Furthermore our lab has demonstrated that an increase in FoxO1 activity blocks hypertrophic growth of cardiac myocytes by decreasing calcineurin activity[37]. Others have shown that calcineurin is a direct target of atrogin-1[58]. Therefore the FoxO transcription factors are ideally positioned as a node between the Akt and calcinuerin pathways, as well as growth and degradation pathways.

In order to study FoxO dependent growth and degradation, I turned to a transgenic mouse model of constitutively active Foxo3a (caFoxo3a) overexpression in skeletal muscle. To this end, mice expressing *Cre* recombinase in muscle (myo-Cre) were crossed with mice transgenic for "Flox-On" caFoxo3a. The myo-Cre transgene's expression is controlled by the mouse myogenin promoter and the skeletal muscle-specific enhancer of the mouse MEF2C gene; it is expressed by embryonic day 9.5 (E9.5) in developing somites[59]. The caFoxo3a construct is rendered active by mutating the three Akt phosphorylation sites to alanine facilitating entry into the nucleus where it can bind to and activate target genes.

The goal of this study was to develop an easily accessible *in vivo* model of muscle growth and degradation that avoided the time and technical expertise required for the TAC pressure overload model.

## Anatomy of the mouse hind limb

The following section provides a brief overview of the anatomy of the mouse hind limb to aid in interpreting the subsequent experimental results. The lower portion of the mouse hind limb is composed of two bones and five muscles (Fig. 3.1). In the anterior aspect is the larger tibia bone, the major weight bearing bone of the lower hind limb. Distally lies the fibula. This smaller bone has evolutionarily been reduced in size and strength. Anterior and medial to the tibia is the tibialis anterior (TA), responsible for dorsiflexion of the foot. The TA muscle functions in walking and running, activities that require the foot to be vertical. Lateral to the TA muscle and posterior to the tibia lies the extensor digitorum longus (EDL) muscle. As the name implies, this muscle functions to extend the digits of the foot and in concert with the intrinsic muscles of the foot, is responsible for fine motor tasks such as grasping and clawing.

The muscles of the posterior compartment of the lower hind limb are the soleus (SOL), plantaris (P), and gastrocnemius (GAS) muscles. Just posterior to the fibula lies the powerful soleus muscle. Immediately posterior to this muscle is the plantaris and further posterior and enveloping the posterior compartment is the larger gastrocnemius. These muscles act to plantarflex the foot. They are essential muscles for walking and running. More importantly these muscle are vital for posture, keeping the hind-portion of the mouse erect.

To function as postural muscles these muscles must be able to contract constantly and resist fatigue. The resistance to fatigue exhibited by these

muscles is aided by the characteristics of the "slow-twitch" fibers that endow them with a high oxidative capacity. These muscles are composed of numerous mitochondria and aerobic respiratory enzymes, and a high concentration of myoglobin. The SOL muscle expresses the highest proportion of these slow-oxidative fibers characterized by the expression of the type I myosin isoform[60]. The GAS muscle also contains some slow-oxidative fibers, predominantly in the medial portion of the muscle. This muscle is the most heterogenous of the muscles in the hind limb in terms of muscle fiber composition. It contains some proportion of the intermediary fast-oxidative fibers, characterized by expression of the type IIa isoform of myosin. Like the muscles of the anterior compartment, the TA and EDL, which are composed almost exclusively of fast-glycolytic fibers, the GAS also contains a high proportion of these fibers. These fibers are characterized by expression of the type IId/x and type IIb isoforms of myosin. These fast-glycolytic fibers are adapted to respire anaerobically by high concentrations of glycolytic enzymes and large glycogen stores. Thus is the biochemical composition of each muscle fiber adapted to its physiologic role.

## Materials & Methods

### Transgenic mice

I am indebted to the investigators that provided the transgenic mice used in this study. Dr. Eric Olson provided the myo-Cre transgenic mouse[59]. Dr. Dian Cao provided the caFoxo3a mouse[61]. The Animal Care and Use Committee of

the University of Texas Southwestern Medical Center at Dallas approved all animal care and procedures.

## Histology

Skeletal muscle were harvested from mice and either flash frozen in embedding medium containing a 3:1 mixture of Tissue Freezing Medium (Triangle Biomedical Sciences, Durham, NC) and gum tragacanth (Sigma, St. Louis, MO) or fixed in 4% paraformaldehyde and processed for routine paraffin histology. Staining for ATPase enzyme activity was carried out as previously described[62]. Paraffin sections were used for H&E staining.

## Myocyte Fiber Cross-sectional Area

Histologic analysis of sections of muscles stained with H&E stain allowed for quantification of cross-sectional area (CSA) of at least 80 individual fibers per muscle group in 5 mice of each phenotype. All images were taken at room temperature and processed in ImageJ for CSA analysis. Occasionally, images were linearly rescaled to optimize brightness and contrast uniformly without altering, masking, or eliminating data.

## Real-time RT-PCR

Total RNA was harvested from mouse TA using TRIzol (Invitrogen) according to the manufacturer's protocol. cDNA was prepared from RNA using a high capacity cDNA reverse transcription kit (Applied Biosystems). Real-time PCR was performed using SYBR green on an ABI 7000 Prism Sequence

Detection System (Applied Biosystems). To confirm amplification specificity, the PCR products were subjected to melting curve analysis. Negative controls containing water instead of cDNA were run concomitantly. Data for each transcript were normalized to reactions performed using GAPDH or 18S rRNA primers, and fold change was determined using the comparative threshold method[38].

## Immunoblot analysis

Skeletal muscle from TA group were either homogenized immediately or quick frozen in liquid nitrogen and stored at −80 °C for later use. To harvest protein, tissues were homogenized at 4°C in M-PER® mammalian protein extraction reagent (Thermo Scientific), with added protease inhibitors (Roche) and phosphatase inhibitors (Sigma). Homogenates were passed over glass wool to remove DNA. Proteins were separated by SDS/PAGE, transferred to a supported nitrocellulose membrane, and immunoblotted. Antibodies for α-tubulin (Sigma-Aldrich), Foxo3a (Sigma-Aldrich), BNIP3 (Sigma-Alrdich), and PGC-1α (Cell Signaling) were used. Blots were scanned, and bands were quantified using Odyssey Licor (version 3.0) imaging system.

## Statistics

Data are presented as mean ± SD or SEM. The unpaired Student's t test was used for comparison between two groups, and ANOVA with Bonferroni correction was used for comparison among multiple groups. Values of $p < 0.05$ were considered significant.

# Results

## Transgenic mice, expressing constitutively active Foxo3a robustly and specifically in skeletal muscle are kyphotic, yet viable

Mice expressing *Cre* recombinase in skeletal muscle (myo-Cre) were bred with mice harboring the constitutively active FoxO3a gene (caFoxo3a). Offspring of this interbreeding were born in expected mendelian ratios. Mice that were double transgenic for the *Cre* recombinase and caFoxo3a (myo-Cre;caFoxo3a) expressed caFoxo3a robustly and specifically in skeletal muscle as demonstrated by immunoblot (Fig. 3.2 A). As early as 6 weeks of age, the myo-Cre;caFoxo3a mice demonstrated a marked over-curvature of the back (Fig. 3.2 B). Otherwise, these mice were viable and could only be distinguished from the control littermates (myo-Cre) by their kyphotic appearance.

## Atrophic response to Foxo3a overexpression is attenuated in muscle groups with more abundant oxidative fibers

To test whether the kyphotic phenotype of the myo-Cre;caFoxo3a could be due to skeletal muscle atrophy, I isolated the muscles of the lower hind limb of these mice and their littermate controls (myo-Cre). Histologic analysis of sections of these muscles stained with hematoxylin and eosin stain (H&E stain) allowed for quantification of cross-sectional area (CSA) of at least 80 individual fibers per muscle group in 5 mice of each phenotype. The TA, EDL and SOL muscles of the myo-Cre;caFoxo3a mice exhibited a marked decrease in CSA when

compared to their littermate controls (CSA, TA, myo-Cre: 1,650 ± 660 $\mu m^2$; myo-Cre;caFoxo3a: 1,140 ± 350, Fig. 3.3 A; EDL, myo-Cre: 2,200 ± 840; myo-Cre;caFoxo3a: 640 ± 160, Fig. 3.3 B; SOL, myo-Cre: 1,980 ± 420; myo-Cre;caFoxo3a: 980 ± 610, Fig 3.3 C; $p<0.05$).

Fibers in the periphery of the GAS were atrophied in response to overexpression of caFoxo3 (CSA, GAS, myo-Cre: 1,440 ± 350 $\mu m^2$; myo-Cre;caFoxo3a: 520 ± 370, $p<0.05$, Fig. 3.3 D). Interestingly the fibers found in the interior of the GAS muscle, just posterior to the soleus muscle were spared from atrophy despite overexpression of caFoxo3a (CSA, GAS, myo-Cre: 1,400 ± 340 $\mu m^2$; myo-Cre;caFoxo3a: 1,360 ± 420, $p<0.05$, Fig. 3.3 D). This portion of the GAS muscle contains the majority of slow-oxidative and fast oxidative fiber types to be found in this muscle, suggesting that fibers of this type are somehow resistant to atrophy induced by overexpression of caFoxo3a.

## Overexpression of Foxo3a increases oxidative fibers

To further investigate this differential response to caFoxo3a overexpression by muscle fiber type, I employed metachromatic ATPase staining to characterize the fiber types preset in the muscle groups. With this technique, fibers with low phosphate (ATP) content, i.e. fast-glycolytic fibers, are stained metachromatically, while fibers of high phosphate (ATP) content, i.e. oxidative fibers, are stained orthochromatically with the intensity of color proportional to the content of insoluble phosphate[62]. When comparing histologic sections from SOL muscle, I noted that consistently, sections from myo-cre;caFoxo3a SOL

contained a higher proportion of orthochromatic fibers when compared to the SOL of myo-cre littermates (Fig. 3.4 A). The other muscles did not show any changes in the proportion of orthochromatic to metachromatic fibers.

The increase in orthochromatic staining in the SOL implied that the muscle is preferentially expressing the slow, oxidative fiber type. To confirm this observation, I performed RT-PCR to quantify expression of the myosin isoforms specific for each fiber type. Indeed, in myo-cre;caFoxo3a SOL muscle, type I myosin expression was increased 2.7-fold ($p<0.05$) over the myo-cre control SOL (Fig. 3.4 B). Type IIb myosin, characteristic of fast-glycolytic fibers, was reciprocally reduced to 0.6-fold of myo-cre control. Type IId/x and type IIa myosin were also increased 2- and 2.3-fold ($p<0.05$), respectively. Taken together, these results demonstrate that overexpression of caFoxo3a changes the composition of the SOL muscle to that of a more oxidative phenotype.

## Overexpression of Foxo3a induces atrogene, metabolic, & differentiation factors

To determine whether proteasomal degradation was responsible for the muscle atrophy in myo-Cre;caFoxo3a mice, I determined whether expression of the atrogenes, *atrogin-1 (Atg1)* and *MuRF1* was increased in the muscle fibers of these mice. These two E3 ubiquitin ligases are known targets of Foxo3a[56, 57]. As determined by RT-PCR, the expression of the *MuRF1* transcript was increased 3.5-fold ($p<0.05$) whereas *Atg1* transcription was not increased significantly (Fig. 3.5 A). This result implies that in this model, skeletal muscle atrophy is

accelerated preferentially through increased ubiquitination of substrates through *MuRF1*.

To determine whether induction of autophagy could also be responsible for the observed skeletal muscle atrophy, I quantified BNIP3 protein levels in skeletal muscle. Although levels of the monomeric form of BNIP3 remained unchanged in myo-Cre;caFoxo3a (Fig. 3.5 D, lower panel), BNIP3 dimer was increased in the skeletal muscle of the mice (Fig. 3.5 D, upper panel). This result indicates that overexpression of caFoxo3a leads to dimerization of BNIP3.

The decreased size of muscle fibers in myo-Cre;caFoxo3a could also be due to a relative inhibition of growth. To answer this question, I measured the transcript of *p21*, a cyclin-dependent kinase and target of the forkhead transcription factors[63], and found that its expression was increased 3.8-fold ($p<0.05$) in the myo-Cre;caFoxo3a skeletal muscle (Fig. 3.5 B). This result indicates that an induction of a cytostatic response was also partially responsible for the skeletal muscle atrophy observed.

Unopposed proteolysis and degradation would lead to complete absence of skeletal muscle fibers, so I determined whether transcription of myogenic factors was activated in myo-Cre;caFoxo3a mice. The myogenic factors, *MyoD (myoD1)* and *myogenin (myoG)* help to control terminal differentiation and establish myoblast identity[64]. The transcipts of these factors were induced in myo-Cre;caFoxo3a skeletal muscle, with *myoD1* expression increased 5.9-fold ($p<0.05$) and *myoG1* expression increased 8-fold ($p<0.05$; Fig. 3.5 C). That

expression of these factors is increased in the myo-Cre;caFoxo3a indicates that muscle differentiation is active in the atrophying muscle as well.

Having shown that transcriptional activation of certain pathways was responsible for the decreased fiber size, I next asked whether this mechanism could explain the change in fiber type observed in the myo-Cre;caFoxo3a skeletal muscle. Expression of PGC-1α (*PGC1a*) promotes mitochondrial biogenesis and oxidative metabolism[65]. In myo-Cre;caFoxo3a skeletal muscle, expression of *PGC1a* was increased 2.1-fold ($p<0.05$; Fig. 3.5 B), but this increase could not be verified at the protein level (Fig. 3.5 D). This result leaves open the possibility that activation of pathways dependent on PGC-1α are responsible for the switch to more oxidative fiber types.

## Discussion

### FoxO3a is an activator of skeletal muscle atrophy

My results confirm that FoxO3a is a potent activator of skeletal muscle atrophy. Previous studies had shown that overexpression of constitutively active FoxO3a (caFoxo3a) in immortalized C2C12 myotubes[66] or in isolated myofibers[56] are sufficient to induce atrophy. I have shown that transgenic overexpression of caFoxo3a in skeletal muscle *in vivo* leads to skeletal muscle atrophy. The cross sectional area of skeletal muscle fiber size in the hind limb of transgenic mice was robustly decreased.

I have shown that FoxO3a induces atrophy by both activating degradation pathways and inhibiting growth. In the atrophying fibers, expression of the E3 ubiquitin ligase *MuRF1* and the cyclin-dependent kinase *p21* were increased, leading to increased proteasome activity and cytostasis, respectively. Interestingly, expression of the other atrogene, *Atg1*, was not increased in the atrophying fibers implying that in this transgenic model increased proteasomal activity is mediated specifically through *MurF1*. It could also be that Atg1 expression was transiently increased and missed in the experimental time frame. Further studies are needed to explain this finding.

Overexpression of caFoxo3a has been shown to activate protein degradation by increasing autophagy[66, 67]. In my studies, I have shown that in the atrophying transgenic skeletal muscle, BNIP3 dimerization is increased. The conserved feature of highly stable dimerization[68] in BNIP3 family members suggests a functional significance, but the precise role of dimerization remains unsolved. Increased expression of BNIP3 has been shown to activate autophagy[22, 69]. Taken together, it is plausible that increased expression of BNIP3 activates autophagy by making more partners available for dimerization, but more studies are needed to support this mechanism.

## Oxidative skeletal muscle is resistant to atrophy

Additionally, my studies suggest that muscle fibers exhibiting the oxidative phenotype are at least partially resistant to atrophy. Fibers found in the interior portion of the gastrocnemius, where this phenotype is more abundant, did

not show a decrease in cross sectional area (CSA) in the transgenic mice. Furthermore, the proportion of oxidative fibers in the soleus muscle of these mice was increased as well, but these fibers did exhibit a decrease in CSA. Increased expression of myogenic differentiation factors (*myoD1* and *myoG1*) and a mitochondrial biogenesis activator (*PGC-1a*) activate a switch to the oxidative phenotype in the transgenic mice. Precisely why these fibers subsequently do not resist atrophy cannot be answered at this point.

## Relevance

In this study I have established an *in vivo* model of skeletal muscle atrophy. Further work with this model to dissect the interplay of growth and degradation pathways, and the role of autophagy therein, could be applicable to that of the heart as well. Understanding how the auotophagy process activated in skeletal muscle atrophy differs from cardiomyocyte autophagy in response to pressure-overload would be an important prerequisite to formulating therapeutics manipulating autophagy to treat heart disease.

## Figures

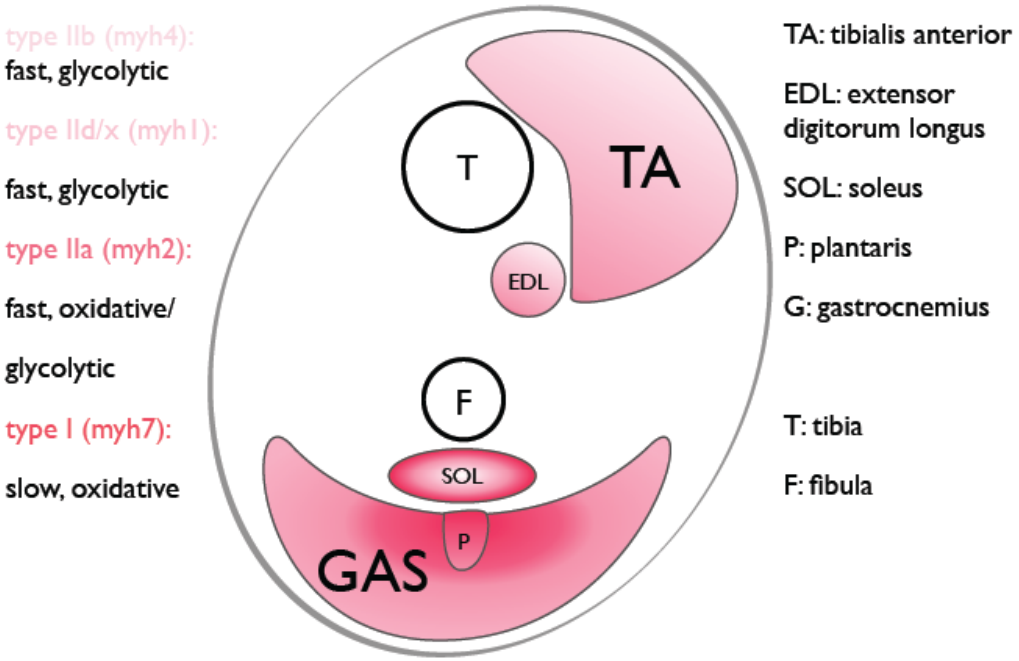


**Figure 3.1. Skeletal muscle in the lower extremity of the mouse has heterogeneous composition.** A diagram of the lower extremity of the mouse shows the various skeletal muscle groups and their relative content of glycolytic and oxidative fibers.


**Figure 3.2. Transgenic mice, expressing constitutively active Foxo3a robustly and specifically in skeletal muscle are kyphotic, yet viable.** (**A**) Immunoblot detection of Foxo3a expression in skeletal muscle. (**B**) Representative images of transgenic mice at 8 weeks age.

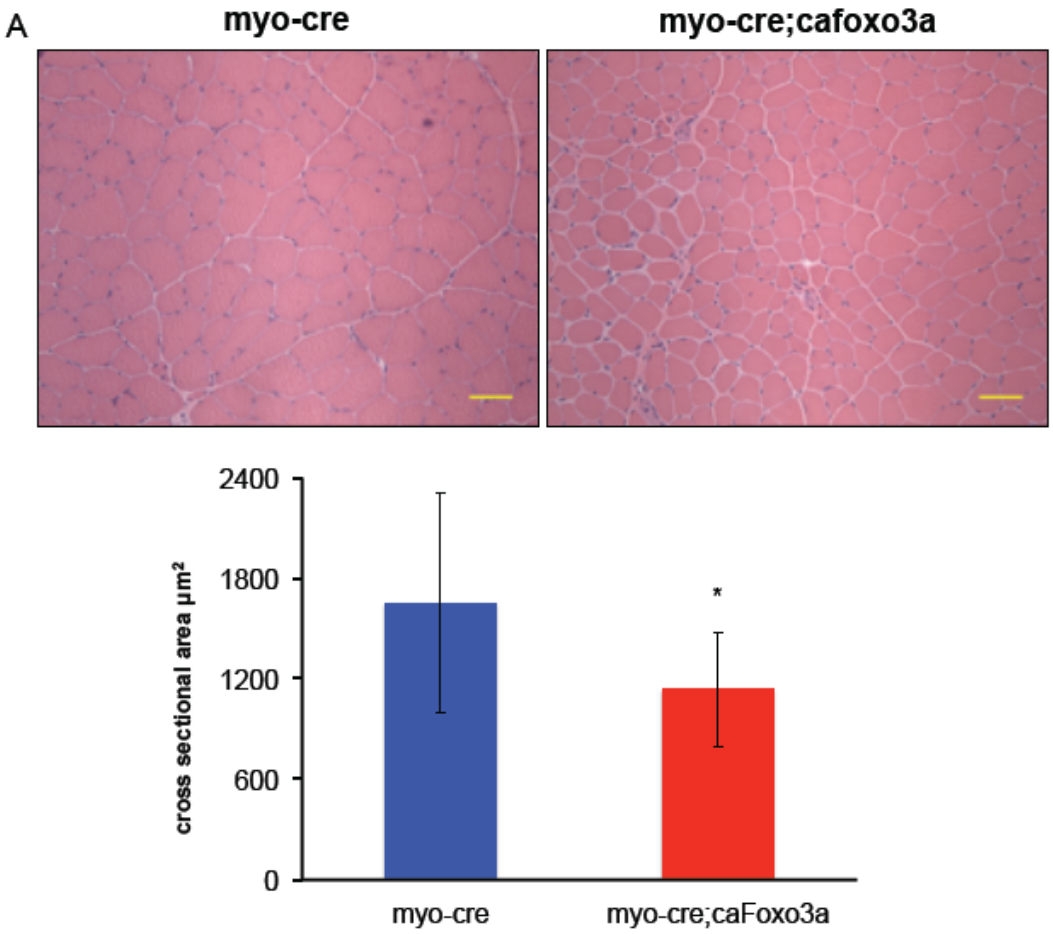


**Figure 3.3. Atrophic response to Foxo3a overexpression is attenuated in muscle groups with more abundant oxidative fibers.** Representative histological sections and quantification of atrophy by cross sectional area in the (**A**) tibialis anterior.

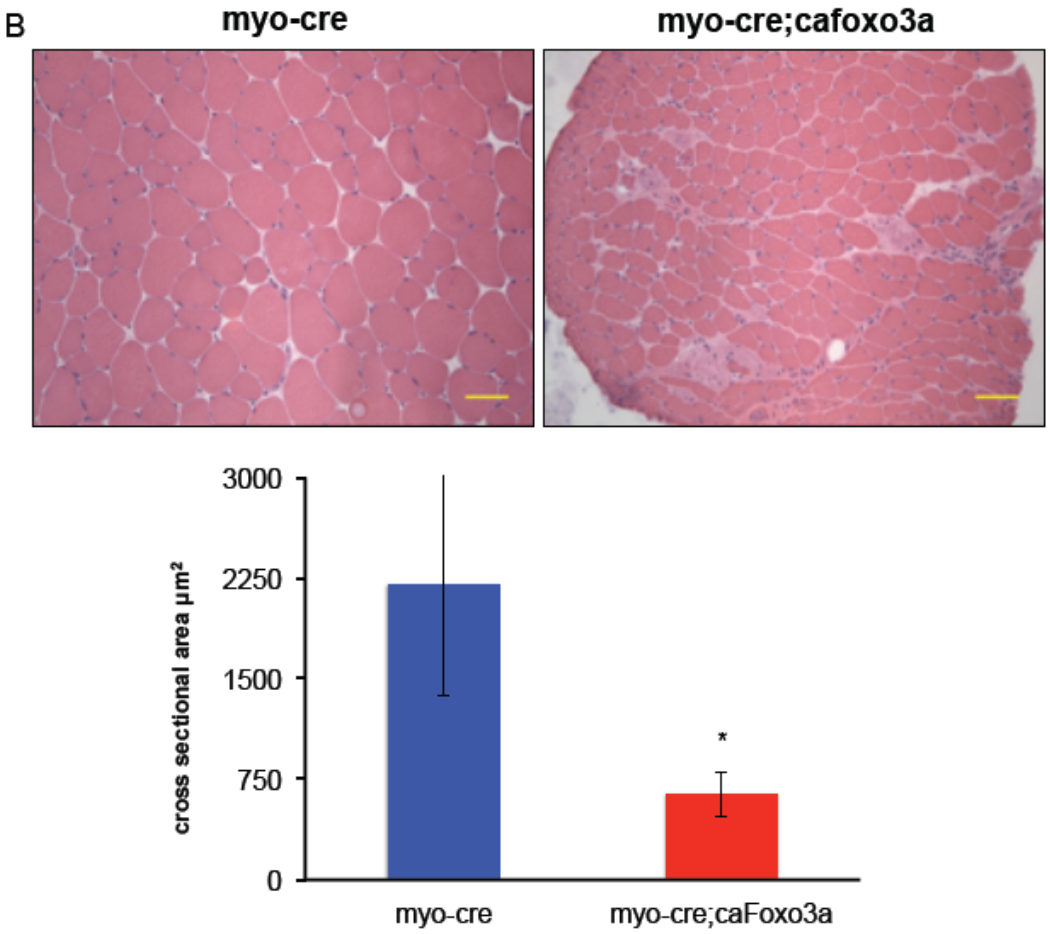


**Figure 3.3 continued.** Representative histological sections and quantification of atrophy by cross sectional area in the (**B**) extensor digitorum longus.

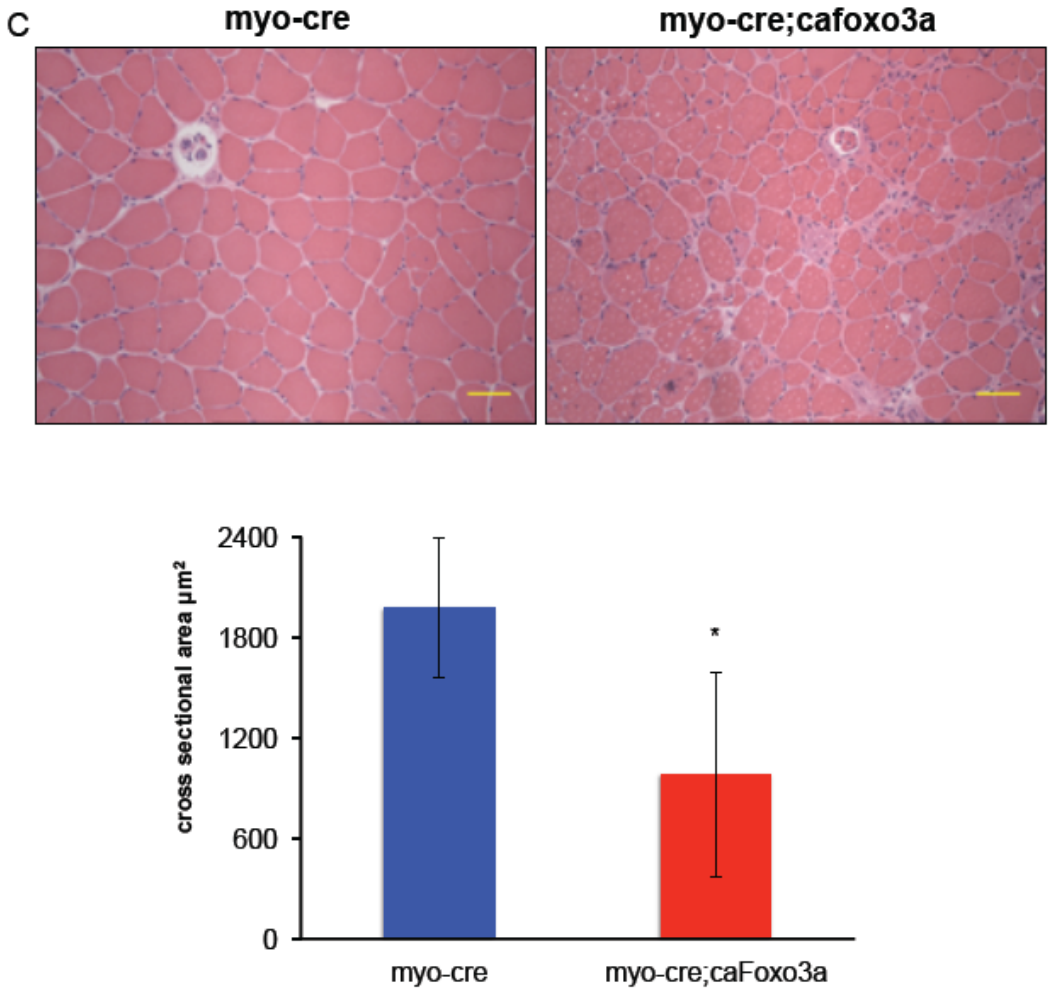


**Figure 3.3 continued.** Representative histological sections and quantification of atrophy by cross sectional area in the (**C**) soleus.

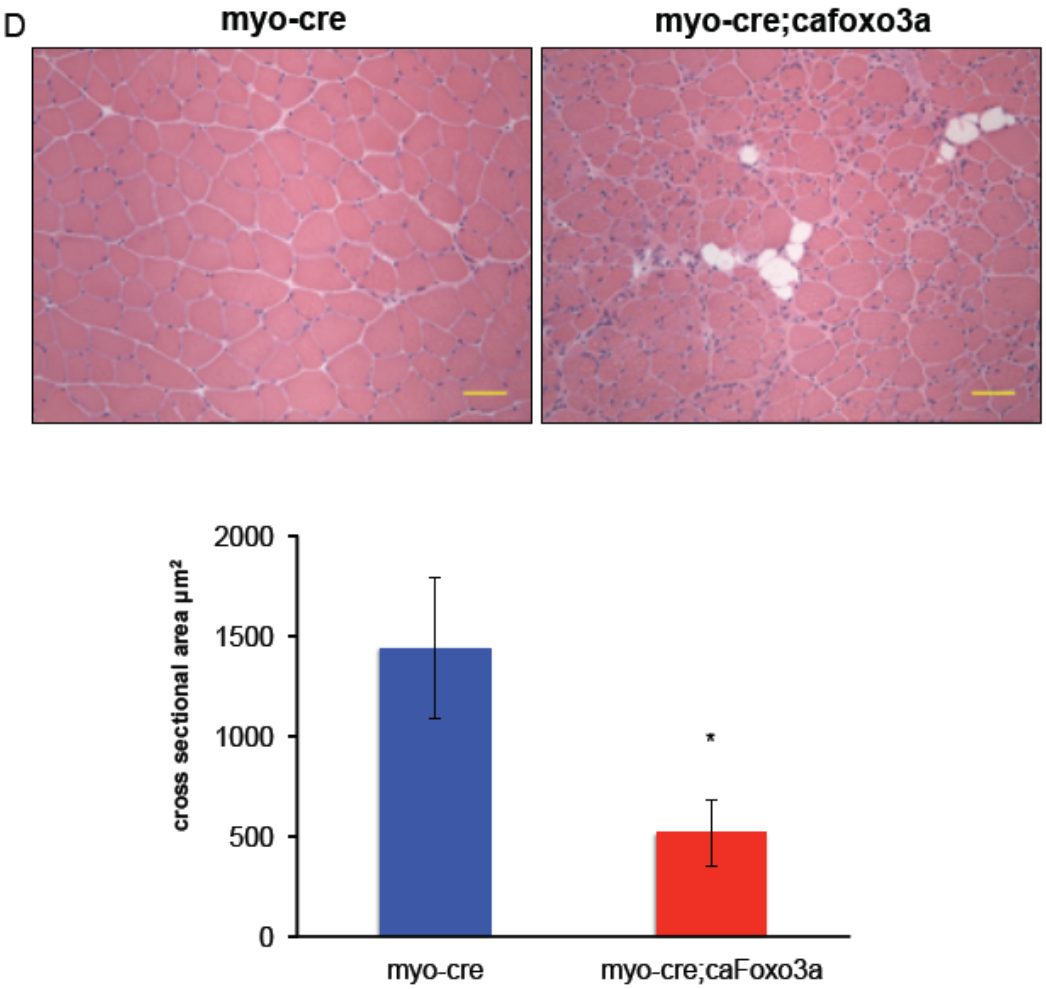


**Figure 3.3 continued.** Representative histological sections and quantification of atrophy by cross sectional area in the (**D**) perimeter of the gastrocnemius.

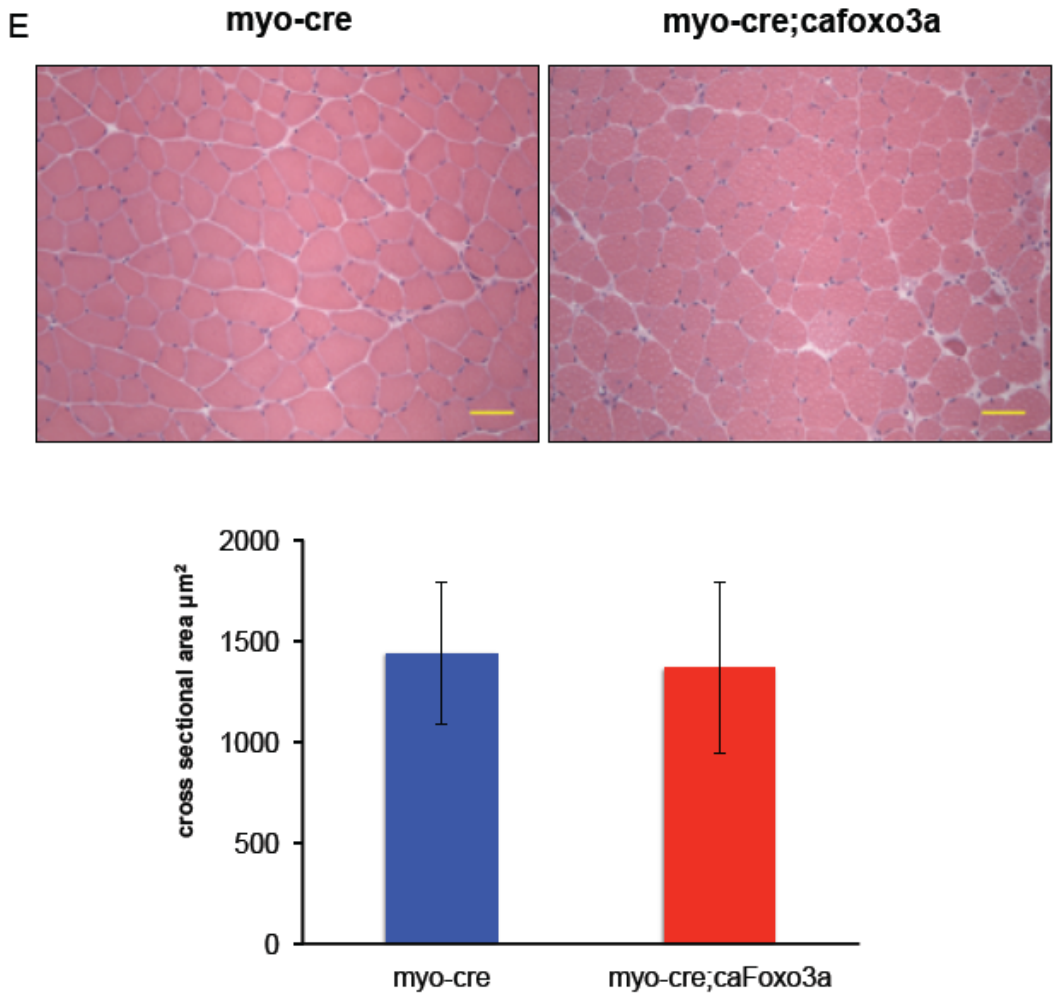


**Figure 3.3 continued.** Representative histological sections and quantification of atrophy by cross sectional area in the (**E**) interior portion of the gastrocnemius.

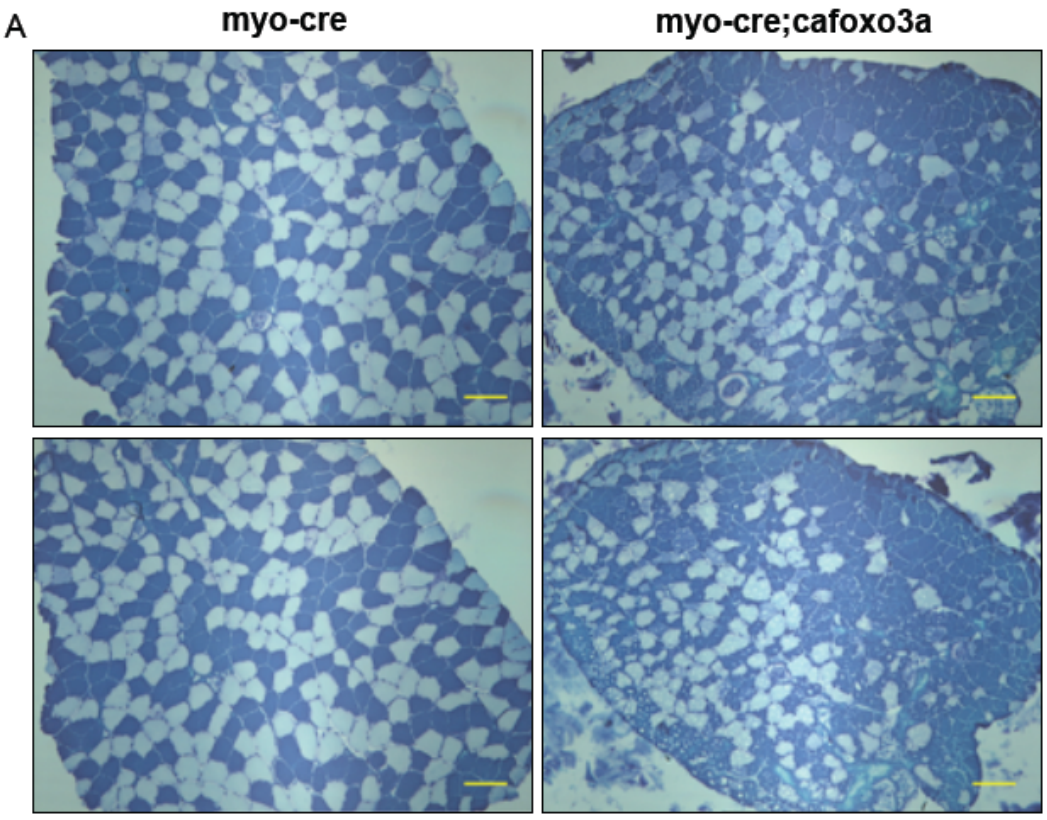


**Figure 3.4. Overexpression of Foxo3a increases oxidative fibers.** (**A**) Metachromatic ATPase staining of soleus fibers shows increased type I fibers.

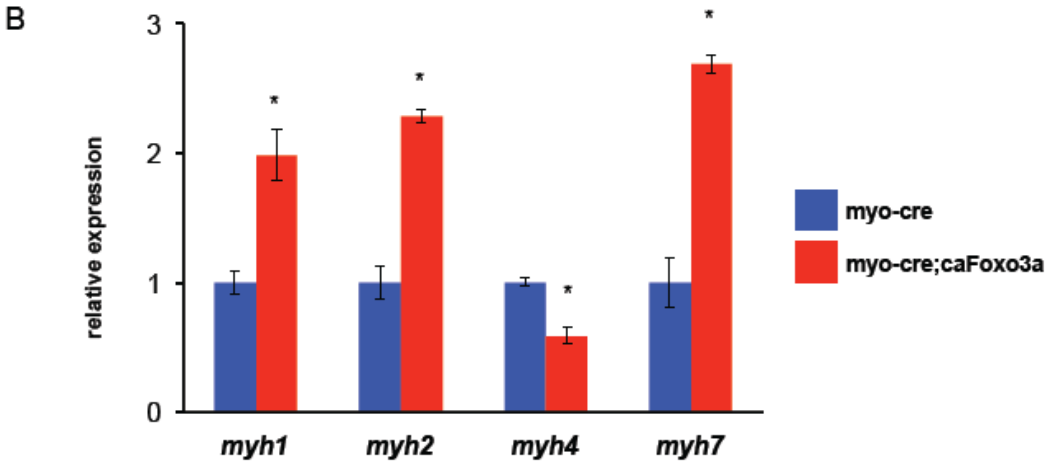


**Figure 3.4 continued.** (**B**) Mean relative mRNA expression in relation to 18s rRNA and normalized to myo-cre levels (*myh1* myosin type IId/x, *myh2* myosin type IIa, *myh4* myosin type IIb, *myh7* myosin type I).

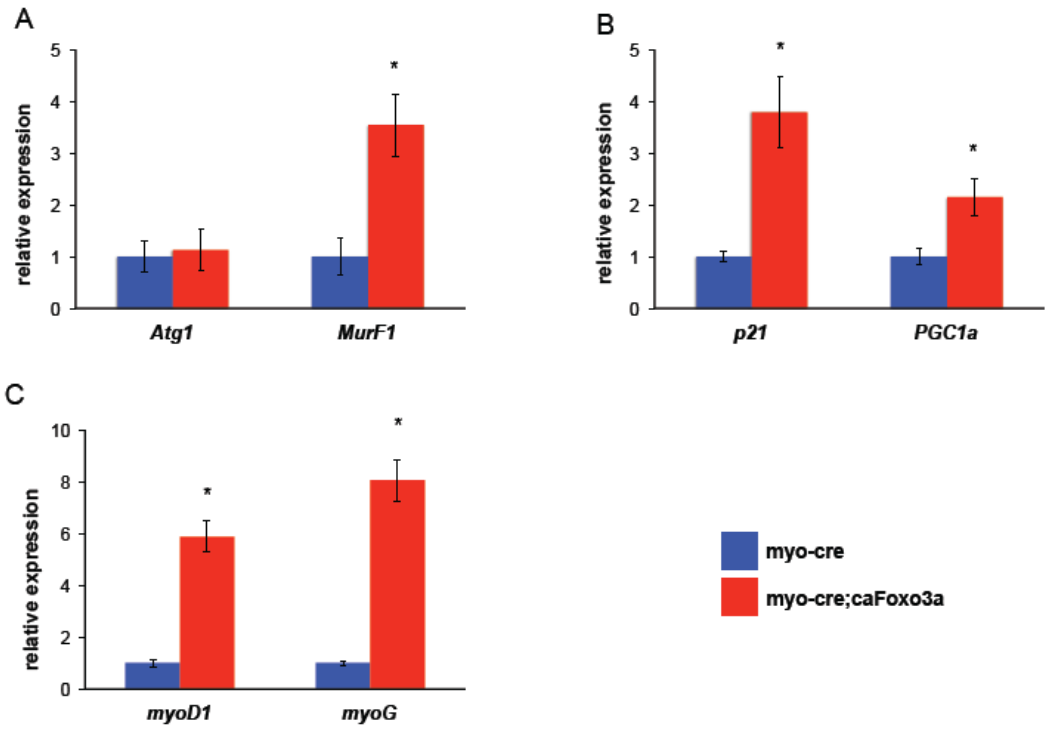


**Figure 3.5. Overexpression of Foxo3a induces atrogene, metabolic, & differentiation factors.** (**A**, **B** & **C**) Mean relative mRNA expression in relation to 18s rRNA and normalized to myo-cre levels.

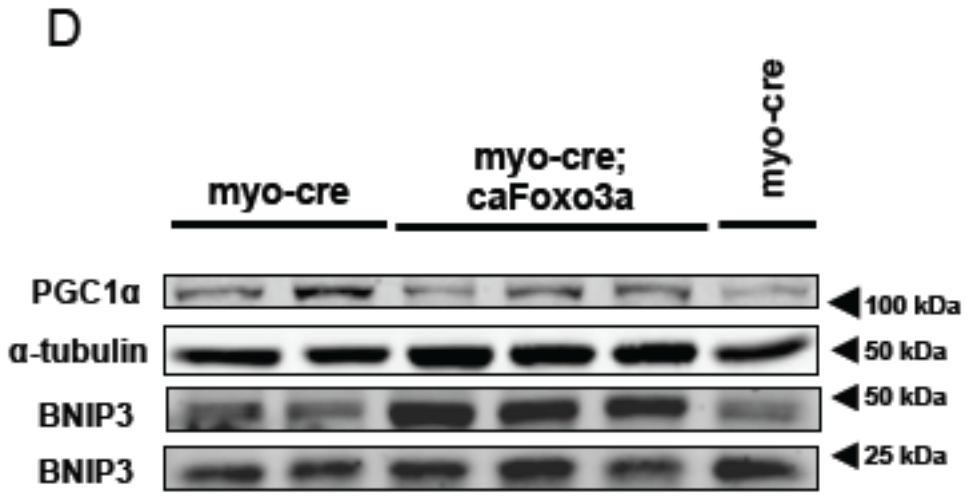


**Figure 3.5 continued.** (**D**) Immunoblot detection of skeletal muscle.

# Chapter 4

# Mitophagy

## Introduction

In eukaryotic cells, mitochondria provide ATP and essential metabolic intermediates for growth, survival, and normal function. This is especially true in the heart, where myosin hydrolyzes ATP to provide energy for muscle contraction. In pathological hypertrophy the rates of ATP hydrolysis and contraction time are decreased resulting in deteriorated cardiac function[70]. This decrease would seem to indicate that mitochondria are either decreased in abundance or rendered dysfunctional. Evidence is conflicting as mitochondrial numbers are increased in several animal models of cardiac hypertrophy[71, 72]. In pressure overload hypertrophy induced by thoracic aortic constriction (TAC) however, concentrations of mitochondrial components, such as cytochrome c, increase after 24h but diminish at 3 days[73].

While oxidative phosphorylation is more efficient at generating ATP than glycolysis, it carries the disadvantage of exposing mitochondria to reactive oxygen species (ROS). Mitochondrial dysfunction subsequently occurs from oxidation of constituent proteins of the electron transport chain (ETC), leading to mitochondrial permeability transition (MPT)[74]. Depolarized mitochondria, having undergone MPT, then generate further ROS[75], thus a vicious cycle is initiated. There are mechanisms by which ROS are scavenged and degraded into non-toxic molecules. Failing that, a specific type of autophagy, mitophagy, clears damaged mitochondria from the cell[76].

In the failing heart, the first description of autophagosomes was accompanied by the observation of mitochondria within them[11]. Subsequently, mitophagy has been extensively characterized in ischemia-reperfusion (I/R) injury. In an experimental model of I/R, autophagic flux was shown to be impaired at the level of induction and degradation and enhancing autophagy was shown to be protective[18]. The role of mitophagy in cardiac hypertrophy has been less studied.

In this study, I first set out to establish an *in vitro* model of cardiac hypertrophy in which mitochondrial abundance and dysfunction could be quantified. Doing so would the allow me to test whether autophagy was necessary for clearing dysfunctional mitochondria in cardiac hypertrophy.

## Materials & Methods

### Mitochondrial dye incorporation

Neonatal rat cardiomyocytes were isolated and cultured as described previously[37]. After 24 hours, NRCMs were transfected with siRNA constructs (Ambion) using Lipofectamine RNAiMax (Invtirogen) in Optimem (Gibco) for 4 hours, and then switched to basal media: DMEM supplemented with 3% fetal bovine serum (FBS), BrdU, and antibiotics. Cultured myocytes were stained with MitoTracker Green or Deep Red (Invitrogen) according to the manufacturer's protocol. Briefly, cultured mycocytes were isolated and centrifuged to obtain a cell pellet. Cells were incubated in basal media containing either 50 nM

MitoTracker Green or 200nM MitoTracker Deep Red for 30 minutes. Cells were again pelleted, washed 3 times in PBS, and resuspended in PBS at a concentration of $10^7$ cells/mL. This suspension was used for flow cytometry. All data were collected on a FACSCalibur flow cytometer (BD Biosciences) and analyzed using FlowJo software (TreeStar).

## Real-time RT-PCR

Total DNA was harvested from NRCMs. Real-time PCR was performed using SYBR green on an ABI 7000 Prism Sequence Detection System (Applied Biosystems). To confirm amplification specificity, the PCR products were subjected to melting curve analysis. Negative controls containing water instead of cDNA were run concomitantly. The relative abundance of mitochondrial DNA to nuclear DNA determined by the ratio of gene product amplified from the mitochondria-encoded gene mtND2 to genomic-encoded gene Mx1.

## Immunoblot analysis

Whole cell lysates from cultured neonatal myocytes were prepared by directly harvesting cells in M-PER® mammalian protein extraction reagent (Thermo Scientific). Proteins were separated by SDS/PAGE, transferred to a supported nitrocellulose membrane, and immunoblotted. Antibodies for α-tubulin (Sigma-Aldrich), Atg5 (Santa Cruz Biotechnology), and p-Drp1 and Drp1 (Cell Signaling) were used. Blots were scanned, and bands were quantified using Odyssey Licor (version 3.0) imaging system.

## Transgenic mice

I am indebted to the investigators that provided the transgenic mice used in this study. The $Atg5^{f/f}$ transgenic mouse was provided by Dr. Noboru Mizushima[14]. The α-MHC-Cre and MCM transgenic mouse lines were provided by Dr. Jefferey Molkentin[77]. The Animal Care and Use Committee of the University of Texas Southwestern Medical Center at Dallas approved all animal care and procedures.

## Echocardiography

Echocardiograms were performed on conscious, gently restrained mice using a Vevo 2100 system with a MS400C scanhead. LVEDD and LVESD were measured from M-mode recordings. FS was calculated as (LVEDD - LVESD)/LVEDD and expressed as a percentage. All measurements were made at the level of the papillary muscles.

## Statistics

Data are presented as mean ± SD or SEM. The unpaired Student's t test was used for comparison between two groups, and ANOVA with Bonferroni correction was used for comparison among multiple groups. Values of $p < 0.05$ were considered significant.

# Results

## Depolarized mitochondria are increased in phenylephrine induced hypertrophy

To test whether growth of cardiomyocytes resulted in an increase of mitochondria, I used the selective α1-adrenergic receptor agonist phenylephrine (PE) and the endothelin receptor agonist Endothelin 1 (ET-1) to induce hypertrophy in neonatal rat cardiomyocytes (NRCMs). I measured the quantity of Mitotracker Green FM dye incorporated into cardiomyocytes by flow cytometry technique. MitoTracker Green FM is a green-fluorescent mitochondrial stain that localizes to mitochondria regardless of mitochondrial membrane potential. Treatment with 50μM PE or 100nM ET-1 did not result in a change in the number of total mitochondria at 24h (Fig. 4.1 A) or 48h (Fig. 4.1 C) as quantified by flow cytometric analysis.

MitoTracker Deep Red is a fluorescent dye that preferentially incorporates into depolarized mitochondria. NRCMs treated with PE and ET-1 for 24h exhibited an apparent increase in depolarized mitochondria when MitoTracker Deep Red incorporation was measured by flow cytometry (Fig. 4.1 B). This increase in depolarized mitochondria was only sustained at 48h in the NRCMs treated with PE and not ET-1 (Fig. 4.1 D).

## Blocking autophagy attenuates the increase in depolarized mitochondria in response to phenylephrine

Next I wanted to investigate whether blocking autophagy would supplement the increase in depolarized mitochondria during cardiomyocyte hypertrophy. Transfecting NRCMs with siRNA directed at Atg5, I was able to knockdown Atg5 protein at both 24h (Fig. 4.2 A) and 48h (Fig. 4.2 B) as demonstrated by immunoblot.

As expected, when NRCMs were treated with PE, the amount of depolarized mitochondria increased as indicated by increased MitoTracker Deep Red intensity at both 24h (Fig. 4.2 C) and 48h (Fig. 4.2 D). Interestingly, blocking autophagy by knocking down Atg5 attenuated the increase in MitoTracker Deep Red intensity seen with PE treatment at 24h (Fig. 4.2 C) and most markedly at 48h (Fig. 4.2 D). This result would seem to indicate that autophagy is necessary for the increase in depolarized mitochondria seen in cardiomyocyte hypertrophy.

## Blocking autophagy attenuates mitochondrial fragmentation in response to PE treatment

To further test whether autophagy was necessary for blocking the decrease in depolarized mitochondria seen in hypertrophied cardiomyocytes, I examined NRCMs with confocal microscopy. The NRCMs were transfected with GFP-LC3 virus to examine autophagic activity and stained with Tetramethylrhodamine, methyl ester (TMRM), a cell-permeant, cationic, red-orange fluorescent dye that is readily sequestered by active mitochondria. As

expected, inducing hypertrophy with PE lead to an increase in autophagy as indicated by increased GFP-LC3 puncta (Fig. 4.3 A). In these NRCMs treated with PE, mitochondria stained with TMRM appeared fragmented and concentrated as seen in a representative image (Fig. 4.3 A).

Autophagy was blocked by the addition of 3-methyladenine (3-MA), a phosphoinositide 3-kinase inhibitor that blocks lysosomal protein degradation, as indicated by decreased GFP-LC3 puncta (Fig. 4.3 A). In these NRCMs treated with PE in which autophagy was blocked, I did not appreciate the appearance of fragmented mitochondria. Rather, these mitochondria appeared elongated and dispersed in a network just as in the control NRCMs.

As an additional measure of mitochondrial abundance, I employed PCR to quantify the relative amount of mitochondrial DNA compared to nuclear DNA in NRCMs. Treating NRCMs with PE resulted in a relative decrease in mitochondrial DNA (Fig. 4.3 B). Blocking autophagy with 3-MA treatment attenuated the relative decrease in mitochondrial DNA seen in NRCMs treated with PE (Fig. 4.3 B). Taken together, these results would suggest that autophagy is necessary for the fragmentation and relative decrease of mitochondria seen in NRCMs induced to hypertrophy by PE.

### Phenylephrine treatment induces Drp1 phosphorylation at serine-616

To explore the mechanism by which autophagy regulates mitochondrial abundance in cardiomyocyte hypertrophy, I tested whether these cellular

processes regulated the phosphorylation of Dynamin-related protein 1 (Drp1). Inducing hypertrophy in NRCMs with PE treatment led to a concomitant increase of phosphorylation of Drp1 at serine-616 at both 24h (Fig. 4.4 A) and 48h (Fig. 4.4 B). Blocking autophagy with siRNA-mediated knockdown of Atg5 did not affect the phosphorylation of Drp1 induced by PE. This result indicates that autophagic regulation of mitochondrial abundance in cardiomyocyte hypertrophy is independent of the mitochondrial fission induction by Drp1.

## Cre;Atg5$^{-/-}$ hearts show similar hypertrophy but diminished function in response to pressure-overload stress

To further investigate the impact of autophagy on mitochondrial dynamics, I turned to a genetic mouse model of autophagy blockade. Mice harboring the floxed allele for *Atg5* (Atg5$^{f/f}$) were crossed with mice expressing the *Cre* recombinase driven by the α-myosin heavy chain promoter (α-MHC-Cre). The eventual offspring of this interbreeding results in a mouse in which autophagy is blocked specifically in cardiomyocytes (α-MHC-Cre;Atg5$^{f/f}$).

I first set out to confirm whether autophagy was necessary for cardiac hypertrophy in response to pressure overload. The hearts of control mice homozygous for the floxed *Atg5* allele (Atg5$^{f/f}$) subjected to thoracic aortic constriction (TAC) showed the expected hypertrophic response as quantified and normalized by heart weight to body weight ratio (HW/BW; Atg5$^{f/f}$, sham: 5.06 ± 0.08 mg/g, n=3; TAC: 7.88 ± 1.3, n=3, $p<0.05$; Fig. 4.5 A). When mice deficient for cardiomyocyte autophagy were subjected to pressure-overload stress, they

also exhibited a comparable hypertrophic response as quantified and normalized by heart weight to body weight ratio (HW/BW; α-MHC-Cre;Atg5$^{f/f}$, sham: 4.91 ± 0.35 mg/g, n=3; TAC: 7.77 ± 0.63, n=3; $p<0.05$; Fig. 4.5 A).

To assess cardiac function, echocardiograms were performed 3 weeks following surgery. Surprisingly, fractional shortening was decreased significantly in the control as well as the autophagy-deficient mice (FS %; Atg5$^{f/f}$, sham: 56.7 ± 8.7%, n=3; TAC: 33.9 ± 3.7, n=3; α-MHC-Cre;Atg5$^{f/f}$, sham: 40.2 ± 2.4, n=3, TAC: 30.0 ± 5.9, n=3; $p<0.05$; Fig. 4.5 B). These functional differences were due to significant increases in both groups of mice in response to pressure-overload stress in left ventricular internal diameter in systole (LVIDs; Atg5$^{f/f}$, sham: 1.2 ± 0.39 mm, n=3; TAC: 2.1 ± 0.38, n=3; α-MHC-Cre;Atg5$^{f/f}$ sham: 1.6 ± 0.14, n=3, TAC: 2.0 ± 0.25, n=3; $p<0.05$; Fig. 4.5 D). Left ventricular internal diameter in diastole was unchanged (LVIDd; Atg5$^{f/f}$, sham: 2.7 ± 0.32 mm, n=3; TAC: 3.1 ± 0.42, n=3; α-MHC-Cre;Atg5$^{f/f}$ sham: 2.8 ± 1.2, n=3, TAC: 2.9 ± 0.60, n=3; $p<0.05$; Fig. 4.5 C). Overall, irrespective of whether autophagy was genetically ablated, mice responded to pressure-overload stress with increased hypertrophy and diminished heart function.

## MCM;Atg5$^{f/f}$ hearts treated exhibit hypertrophy and diminished function in response to tamoxifen treatment

As an alternative genetic mouse model for autophagy ablation, I employed a temporally controlled cardiac-specific deletion of Atg5 to block cardiomyocyte autophagy. To this end, I crossed mice homozygous for the floxed

allele of *Atg5* (Atg5$^{f/f}$) with transgenic mice expressing the *Cre* recombinase in a tamoxifen-inducible and cardiomyocyte-specific manner (MCM). The eventual resulting mice (MCM;Atg5$^{f/f}$) were given intraperitoneal injections of tamoxifen (50 mg/kg) for three days in order to delete the *Atg5* gene. Littermate controls only bearing the floxed allele (Atg5$^{f/f}$) were treated in a similar manner.

Six days after completion of tamoxifen injection, the hearts from the autophagy-deficient mice displayed marked hypertrophy as quantified and normalized by heart weight to body weight ratio (HW/BW; Atg5$^{f/f}$: 4.69 ± 0.11 mg/g, n=3; MCM;Atg5$^{f/f}$: 6.54 ± 1.6, n=3; $p<0.05$; Fig. 4.6 A). In assessing cardiac function, it was determined that after tamoxifen injection, the MCM;Atg5$^{f/f}$ hearts showed a statistically significant decline in cardiac function as quantified by fractional shortening (FS %; Atg5$^{f/f}$, pre: 51.8 ± 2.4%, n=3; post: 55.8 ± 1.8, n=3; MCM;Atg5$^{f/f}$, pre: 49.6 ± 5.3, n=3, post: 27.5 ± 4.5, n=3; $p<0.05$; Fig. 4.6 B). This functional difference was due to a significant increase in left ventricular internal diameter in systole (LVIDs; Atg5$^{f/f}$, pre: 1.3 ± 0.21 mm, n=3; post: 1.2 ± 0.05, n=3; MCM;Atg5$^{f/f}$ pre: 1.3 ± 0.01, n=3, post: 2.1 ± 0.24, n=3; $p<0.05$; Fig. 4.6 D). Left ventricular internal diameter in diastole was unchanged (LVIDd; Atg5$^{f/f}$, pre: 2.6 ± 0.30 mm, n=3; post: 2.8 ± 0.01, n=3; MCM;Atg5$^{f/f}$ pre: 2.6 ± 0.04, n=3, post: 2.9 ± 0.51, n=3; $p<0.05$; Fig. 4.6 C). Taken together, these results indicate that tamoxifen induced genetic ablation of Atg5 to render cardiomyocytes autophagy-deficient results in cardiac hypertrophy and diminished cardiac function as soon as 6 days.

## Discussion

I have demonstrated that the total number of mitochondria is not altered in NRCMs treated with two different hypertrophic agonists (PE and ET-1). Rather, PE, and not ET-1, selectively increases the number of depolarized mitochondria in cardiomyocytes. Both agonists bind to G protein-coupled receptors (GPCRs) of the subtype $G_q$ coupled receptor, to activate phospholipase C and augment $Ca^{2+}$ release into the cell[78]. $Ca^{2+}$ overload is a key activator of MPT[79]. I surmise that NRCMs activate ROS scavenging mechanisms preferentially in response to ET-1, protecting the mitochondria from depolarization, but of course, further studies are needed.

An unexpected finding was that blocking autophagy by knocking down the essential autophagy gene *Atg5* resulted in an attenuation of the increased depolarized mitochondria seen in response to PE treatment. Similarly, blocking autophagy pharmacologically with 3-MA prevented the appearance of fragmented, and presumably depolarized mitochondria in response to PE treatment. These findings suggest that autophagy is at least less than essential for the removal of depolarized mitochondria or may even be required for depolarizing mitochondria. Another possibility is that the autophagy-deficient cardiomyocytes have adapted to increase ROS-scavenging mechanisms leading to a decrease in depolarized mitochondria. Additional studies would need to take into account these other pathways in order to understand the importance of autophagy in mitochondrial homeostasis.

One insight into the mechanism of mitochondrial depolarization induced by PE treatment was that Drp1 phosphorylation in these cardiomyocytes. Drp1 is a GTPase that is required for mitochondrial fission and its recruitment to mitochondria is facilitated by phosphorylation[80]. Presumably, activation of mitochondrial fission by this mechanism would explain the appearance of fragmented mitochondria in NRCMs treated with PE. Blocking autophagy, at least by knocking down *Atg5*, did not have an effect on Drp1 phosphorylation, thus modulation of this pathway cannot explain attenuation of mitochondrial fragmentation or depolarization.

An effective *in vitro* model must be able to replicate *in vivo* findings. In this case, the transgenic mouse line in which the *Atg5* gene has been genetically ablated would provide the *in vivo* model to which to compare. My initial characterization of these mice found that even at baseline, the mice deficient for *Atg5* exhibited diminished heart function. To investigate the role of mitochondrial dynamics in this *in vivo* model, I would propose to quantify mitochondria by PCR to compare the relative amount of mitochondrial DNA compared to nuclear DNA. Then I could begin determining if alterations in mitochondrial dynamics could be responsible for the cardiac hypertrophy and dysfunction seen in these mice.

## Figures

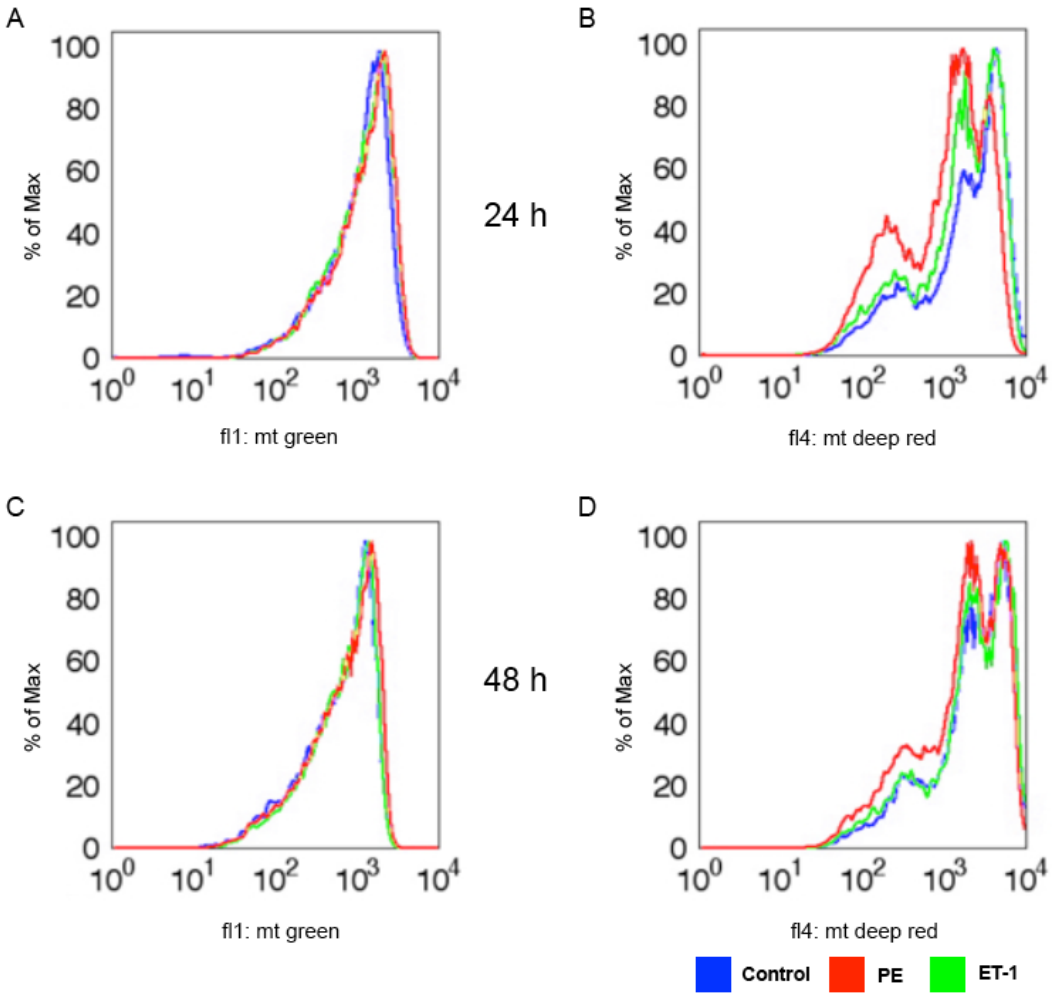


**Figure 4.1. Depolarized mitochondria are increased in phenylephrine induced hypertrophy.** Histograms quantifying flow cytometry analysis of NRCMs treated with vehicle control (Control), 50μM phenylephrine (PE), or 100nM endothelin1 (ET-1) for 24h (**A** & **B**) or 48h (**C** & **D**) and stained with Mitotracker Green (**A** & **C**) or Mitotracker Deep Red (**B** & **D**).

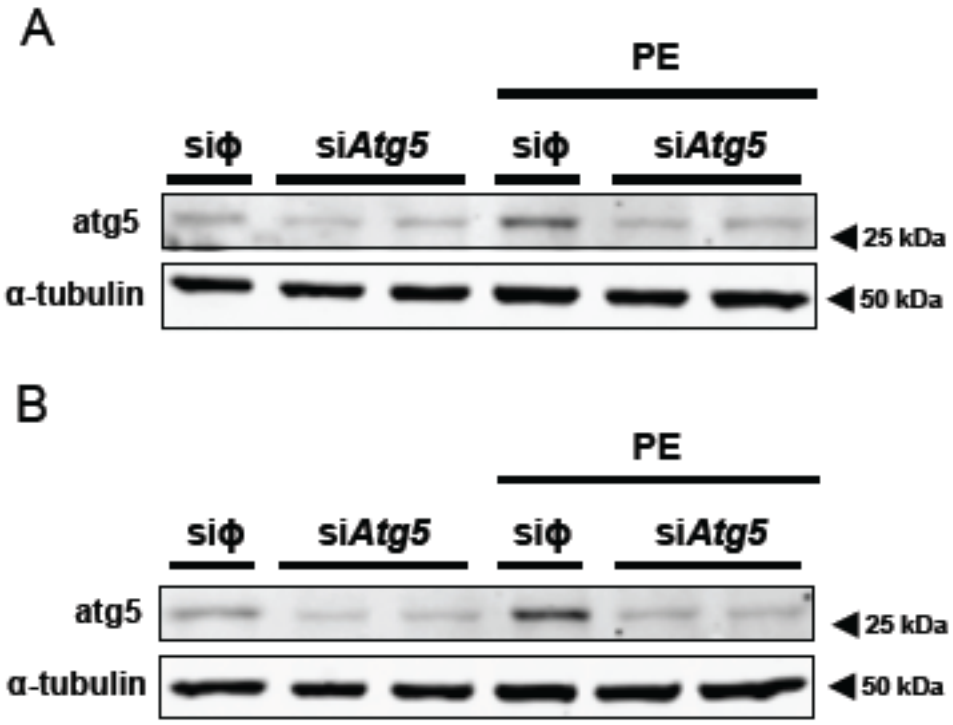


**Figure 4.2. Blocking autophagy attenuates the increase in depolarized mitochondria in response to phenylephrine.** Immunoblot detection of NRCMs after 24h (**A**) or 48h (**B**) of siRNA mediated knockdown, with or without treatment with PE.

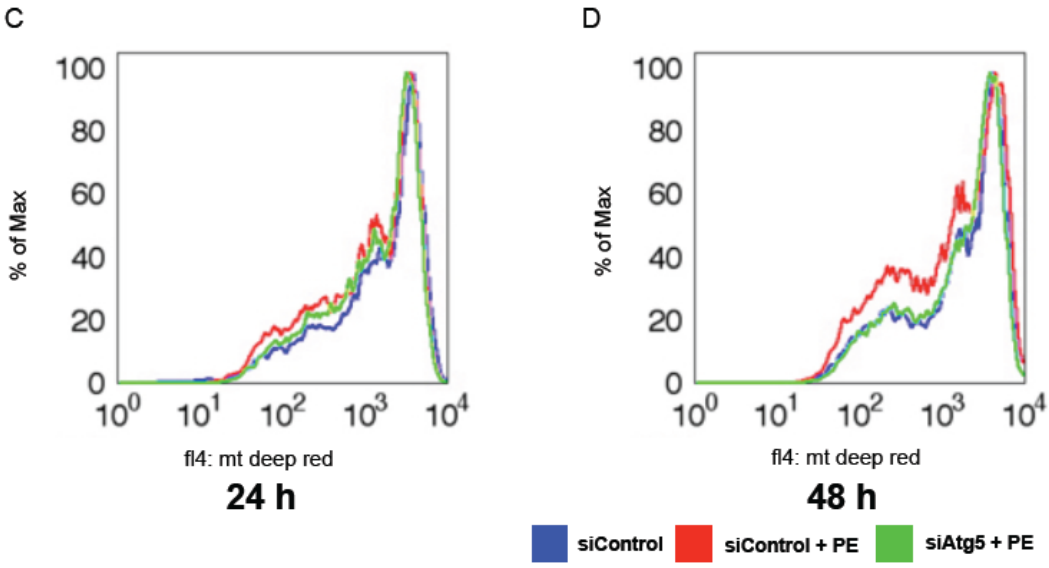


**Figure 4.2 continued.** Histograms quantifying flow cytometry analysis of NRCMs after 24h (**C**) or 48h (**D**) of siRNA mediated knockdown, with or without treatment with PE and stained with Mitotracker Deep Red.

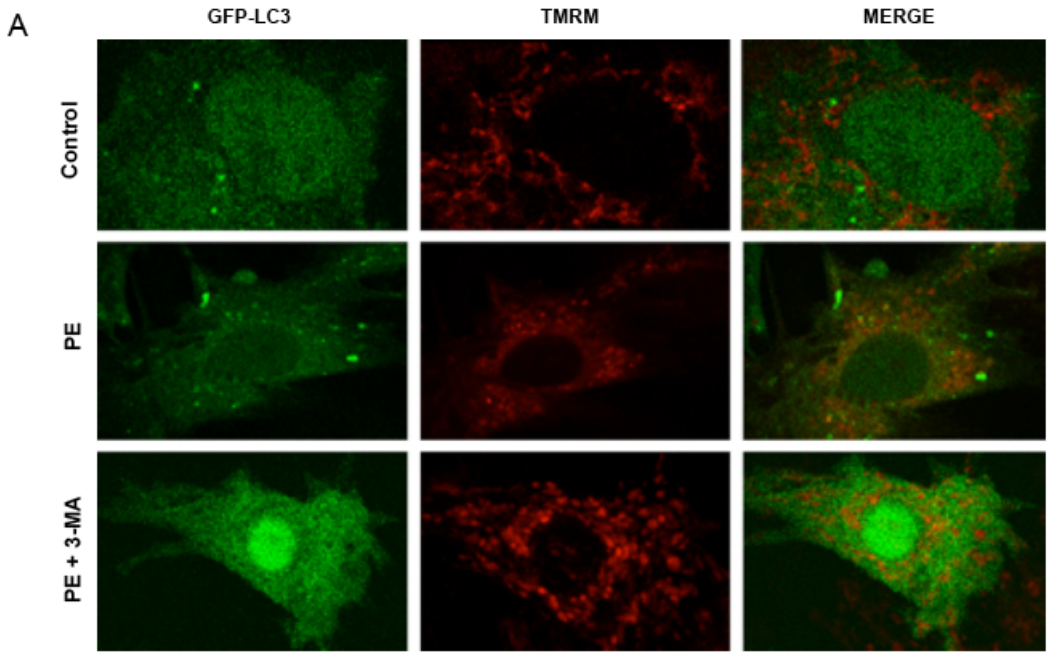


**Figure 4.3. Blocking autophagy attenuates the fragmentation and decrease in mitochondrial DNA in response to PE treatment.** Representative images of NRCMs expressing GFP-LC3 virus and stained with TMRM treated with vehicle control, PE, or PE and 3-MA after 24h (**A**).

B

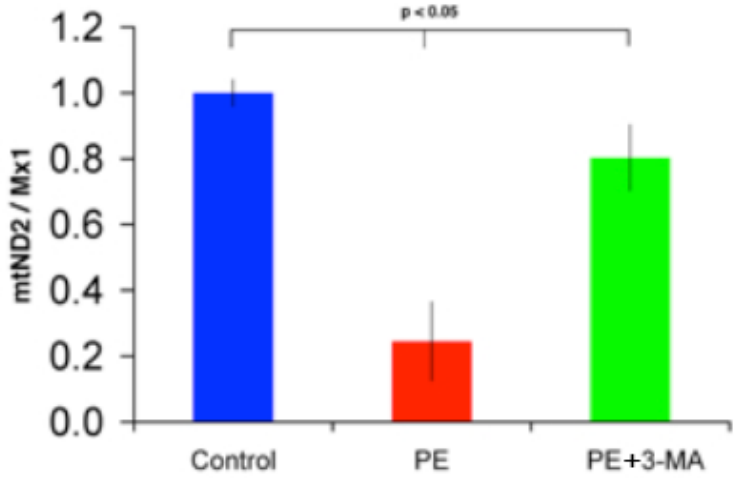


**Figure 4.3 continued.** Relative quantification of mitochondrial DNA with respect to nuclear DNA (**B**).

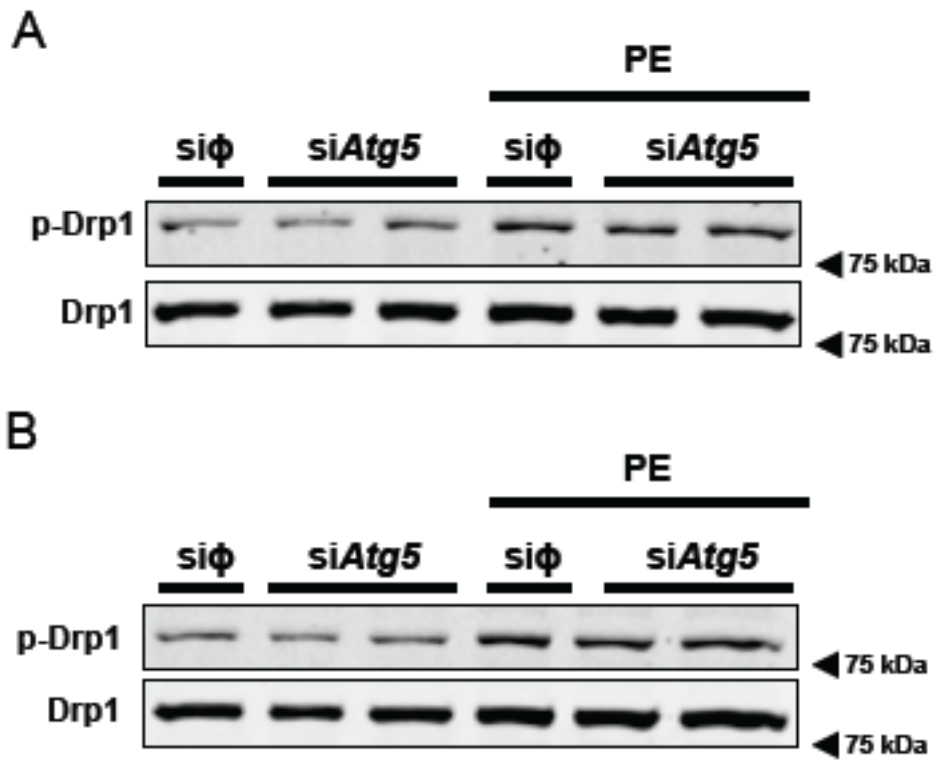


**Figure 4.4. Phenylephrine treatment induces Drp1 phosphorylation at serine-616.** Immunoblot detection of NRCMs after 24h (**A**) or 48h (**B**) of siRNA mediated knockdown, with or without treatment with PE.

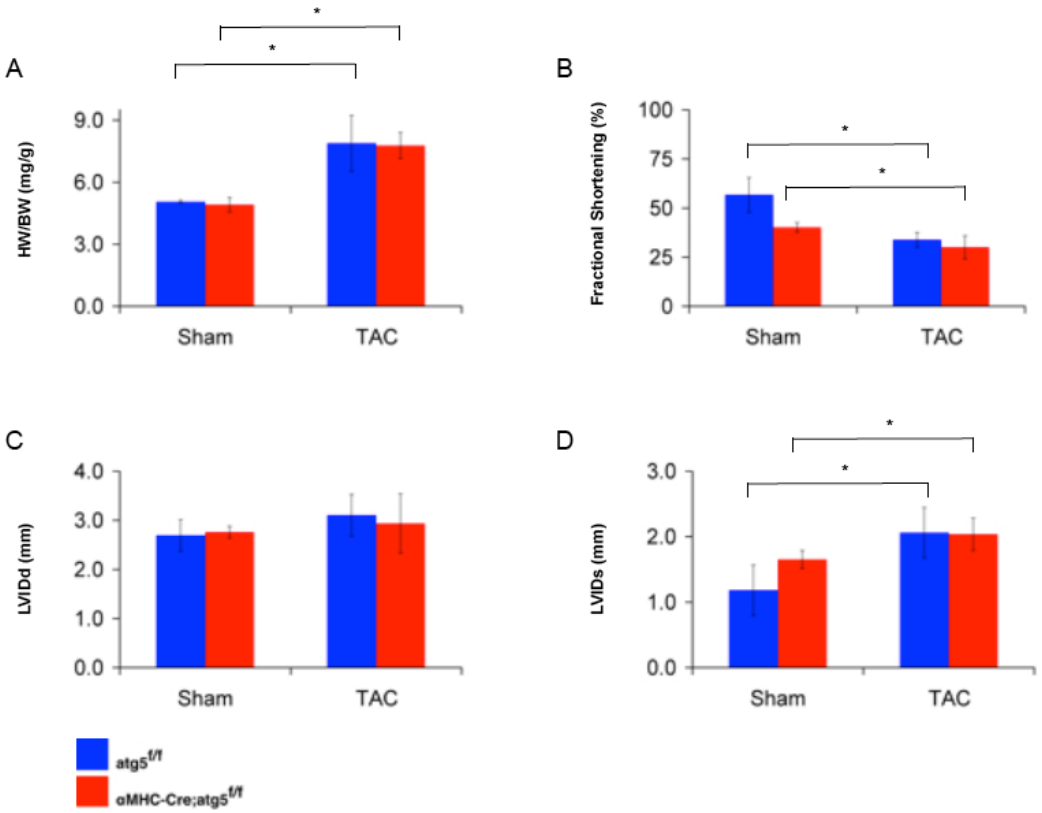


**Figure 4.5. α-MHC-Cre;Atg5$^{f/f}$ hearts show similar hypertrophy and diminished function in response to pressure-overload stress.** The growth response was quantified and normalized by heart weight to body weight ratios (**A**). Heart function represented by (**B**) Fractional shortening (**C**) Left ventricular internal diameter in diastole (mm). (**D**) Left ventricular internal diameter in systole (mm).

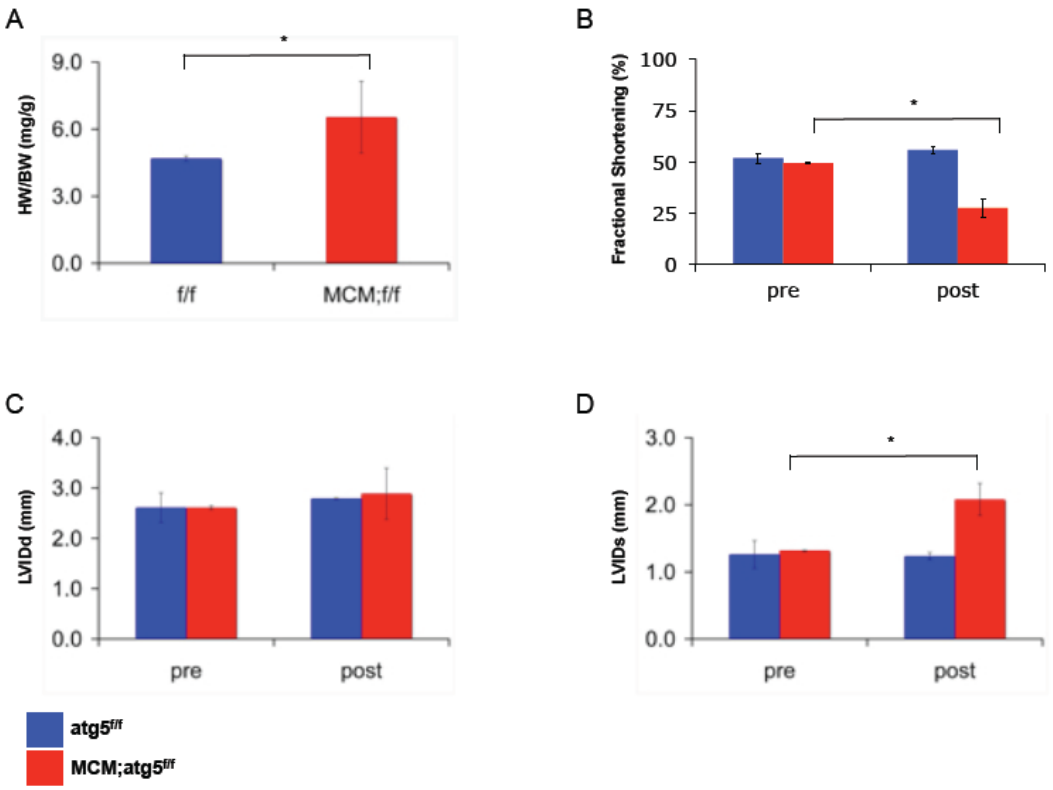


**Figure 4.6. MCM;Atg5$^{f/f}$ hearts treated exhibit hypertrophy and diminished function in response to tamoxifen treatment.** The growth response was quantified and normalized by heart weight to body weight ratios (**A**). Heart function represented by (**B**) Fractional shortening (**C**) Left ventricular internal diameter in diastole (mm). (**D**) Left ventricular internal diameter in systole (mm).

# Chapter 5

# Conclusions & Future Directions

## Rationale

Cardiovascular disease (CVD) remains the leading cause of morbidity and mortality in the United States even though death rates attributable to CVD have declined[81]. Understanding the molecular mechanisms behind myocardial remodeling provide the best hope for being able to therapeutically alleviate this disease burden. To this end, the Hill laboratory, among others, has provided evidence for autophagy as a major player in the remodeling response.

What I found most interesting, was that both cardiac hypertrophy and autophagy exhibited a dichotomous role in heart failure. Cardiac hypertrophy seemed to be a short-term adaptation to normalize wall stress in response to pressure overload, but in the long run, it predisposed the individual to heart failure. Autophagy also appeared to be a beneficial immediate response to the increase in energy demands, but if left unchecked, perhaps it led to irreversible damage. So to uncover what role autophagy played in the hypertrophic response, I looked to see what else these two processes shared and that was the requirement of both for a source of membranes. Autophagic vacuoles are composed of membranes and a hypertrophying cardiomyocyte needs to deliver membranes to the sarcolemma in order to grow.

Recent work had demonstrated a role for the exocyst in autophagosome assembly. The small G protein, RalB, and an Exo84-dependent subcomplex of the exocyst were demonstrated to be critical for nutrient starvation and pathogen-induced autophagosome formation[33]. The exocsyt had a role in membrane

delivery in polarized epithelial cells as well[33]. Thus activation of the exocyst seemed to be a plausible node for the mechanism of inducing cardiomyocyte autophagy and cardiac hypertrophy.

## RalGDS is essential for cardiomyocyte autophagy

My studies focused on the necessity of RalGDS, a guanine exchange factor (GEF) for the Ral subfamily of small GTPases. But first, I confirmed that RalB was indeed similarly responsible for mobilizing autophagic flux in cardiomyocytes as well. *In vitro* studies in NRCMs showed that RalB was necessary for starvation-induced and pharmacologically-induced autophagy.

RalGDS was similarly necessary for autophagy. The autophagic response was blunted in NRCMs knocked down for RalGDS, although not as greatly as those lacking RalB. This could be explained if other GEFs may also engage RalB to mobilize the autophagic response. The direct interplay of RalGDS with RalB remains to be tested, especially whether RalGDS unequivocally activates RalB in response to starvation for example.

## RalGDS is necessary for cardiac hypertrophy

More importantly, cardiac hypertrophy induced by pressure overload is dependent upon RalGDS. Mice subjected to TAC showed a diminished autophagic response to the procedure. RalGDS$^{-/-}$ hearts did not hypertrophy and maintained normal heart function by echocardiography. Thus my study is another

preclinical example of the dispensability of cardiac hypertrophy for preserved heart function in response to stress.

Interestingly, loss of RalGDS was not sufficient to protect from hypertrophy induced by more severe forms of pathological stress. Initial results I gather showed that RalGDS$^{-/-}$ mice subjected to severe thoracic aortic constriction (sTAC) or expressing a constitutively active form of calcineurin (CnA*) showed similar hypertrophic response as the wild type controls. I would like to follow up to examine the autophagic response in these mice. Could it be that severe stress signals can activate different or multiple pathways to activate autophagy?

## A role for RalGDS in physiological hypertrophy?

There is evidence that RalGDS can function as a molecular scaffold for Akt activation[82] and Akt is known to be a mediator of physiological cardiac growth[83]. I have preliminary evidence suggesting that Akt activation in response to refeeding after starvation was impaired in the RalGDS$^{-/-}$ mice. An intriguing experiment would be to see the response of these mice to a physiological model of cardiac hypertrophy such as free-wheel running. This may provide an interesting tool for probing the differences between physiological and pathological hypertrophy. RalGDS-dependent cardiomyocyte autophagy is a valuable tool to probe some of these more general unanswered questions in cardiac remodeling.

## Autophagy in skeletal muscle atrophy

Another interesting dichotomy of autophagy: it is activated in the setting of both cardiac hypertrophy[24] and atrophy[84]. I chose to investigate autophagy in skeletal muscle atrophy however as this was a more technically accessible model compared to the expertise required for TAC and mechanical unloading. To this end I established a transgenic mouse model for muscle-specific overexpression of caFoxO3a. I was able to confirm the findings of previous studies that relied on either immortalized cell lines[66] or electroporation of isolated muscle fibers[56]. Namely that FoxO3a induces skeletal muscle atrophy by activating both proteasomal degradation and autophagy.

A significant finding of my study is the increased abundance of BNIP3 dimer in the atrophying skeletal muscle of the transgenic mice. Indeed, BNIP3 appears to be a key regulator of autophagy and proposed mechanisms of action include generation of reactive oxygen species (ROS)[22] and through interference of the inhibitory Beclin 1-Bcl-2 complex[85]. I postulate that BNIP3 dimerization is a mechanism for activating autophagy. Further examination of this hypothesis could be undertaken by testing whether overexpression of BNIP3 isoforms harboring mutations in the homodimerization domain could block the autophagy in the myoCre;caFoxo3a transgenic model.

## Oxidative skeletal muscle is resistant to atrophy

Two other interesting observations made in this transgenic model are that oxidative fibers of the interior portion of the gastrocnemius muscle (GAS) did not

atrophy and that the proportion of oxidative fibers in soleus muscle (SOL) was increased. There is precedent for fiber-specific atrophy based on the stimulus for skeletal muscle atrophy. Oxidative fibers are sensitive to atrophy induced by denervation[86], whereas glycolytic fibers preferentially atrophy in fasting[87] and cancer cachexia[88]. Furthermore, in skeletal muscle specific FoxO1 knockout mice, fiber type distribution favored the glycolytic phenotype at the expense of oxidative fibers[86]. Therefore the converse, increased oxidative fibers, would be expected with Foxo3a overexpression as I have demonstrated.

The increased transcription of *PGC1a* in the skeletal muscle expressing caFoxo3a is a plausible mechanism for these observations. Transgenic expression of PGC-1α in skeletal muscle has been shown to induce the fiber-type switch by increasing expression of mitochondrial oxidative metabolism[65]. Also, transfection of PGC-1α into isolated muscle fibers reduces the capacity of FoxO3a to cause atrophy by blocking its binding to the atrogin-1 (*Atg1*) promoter[89]. Interestingly the myoCre;caFoxo3a SOL muscle fibers, where fiber-type switch was observed, did exhibit atrophy. I propose that increased *PGC1a* expression is sufficient to activate the fiber-type switch, but does not inhibit the autophagy-dependent atrophy in these fibers. To possibly test this hypothesis, I would need to first demonstrate differential activation of autophagy specific to fiber type. Then, further studies where autophagy is abrogated by siRNA electroporation into the skeletal muscle would be required.

## Inconsistencies of mitophagy

Mitochondria were an intriguing possibility as the target of cardiomyocyte autophagy in cardiac hypertrophy. Extensive work had been done in ischemia-reperfusion models, but mitophagy in the context of pressure-overload hypertrophy was neglected. I thought that agonist-induced hypertrophy of NRCMs would be a robust model in which to study mitophagy. In this model, I could use various pharmacological agonists, manipulate autophagy both genetically and pharmacologically, and measure mitochondrial abundance with various techniques. Unfortunately inconsistencies emerged in all three of these facets, complicating this project, and essentially rendering it inconclusive at this point.

A novel technique I attempted to introduce to our lab was the use of flow cytometry to quantify incorporation of mitochondrial dyes in NRCMs. In using two different dyes, one specific to depolarized mitochondria and one that bound to all mitochondria, I wanted to quantify both abundance and damage. I initially discovered that total mitochondrial abundance was presumably unaltered in response to most hypertrophic-agonists. In the experiments utilizing MitoTracker Deep Red, I showed that depolarized mitochondria abundance was specifically affected by PE treatment. In these experiments however, results could be inconsistent. For example, in some instances, treatment with PE for 24 hours was sufficient to demonstrate an increase in depolarized mitochondria (Fig. 4.1 B), whereas at other times it did not (Fig 4.2 C). I believe a large contributor to

these inconsistencies was the procedure of staining the cells themselves. The staining had to be done in suspension and the procedure lasted 30 minutes. The NRCMs are just too fragile a cell to withstand the rigors of this procedure. I considered fixation of the cells, but MitoTracker Green is not suitable for fixed cells. These inconsistencies lead me to conclude that using flow cytometry to quantify mitochondrial dyes in NRCMs is not yet an acceptable method for studying mitophagy in cardiomyocytes.

## Modeling cardiac hypertrophy

A major challenge that I found myself addressing with each of the projects described in this thesis was establishing a good *in vitro* model representative of the TAC mouse model. The TAC model is technically challenging and for consistent results repetition is needed in the hands of a skilled operator. With the "Foxo3a Controls Skeletal Muscle Atrophy" project I turned away from cardiomyocytes altogether. In the other two projects however, I attempted to model cardiac hypertrophy in NRCMs by treating with pharmacological agonists.

The first question that arises is which agonist to choose for this purpose. An impressive number of molecules have been identified as stimuli for cardiac hypertrophy[8] and likely it is an interplay of all these factors that contribute to the observed response. I consistently employed PE as my agonist-of-choice to induce hypertrophy in NRCMs, but as demonstrated in the "Mitophagy" study, treating with ET-1 had a differential effect on depolarized mitochondrial abundance in NRCMs. In the "RalGDS" project, when trying to quantify

hypertrophy in NRCMs knocked down for RalGDS, RalA, RalB using a radioactive leucine incorporation assay, I was unable to get consistent results. I believe that using one pharmacologic agent to induce hypertrophy in NRCMs is too reductionist of a method for modeling cardiac hypertrophy.

Perhaps one of the more glaring weaknesses of the NRCM *in vitro* model is that they are neonatal cells. The current accepted paradigm for cardiac hypertrophy is the reactivation of the fetal gene program[90]. It would seem counterintuitive to study these pathways in a primary cell line derived from a mouse so early in development. We try to get around this problem by borrowing the technique of serum-withdrawal, which has been shown to induce differentiation of skeletal myoblasts[91], before adding pharmacologic agonists of hypertrophy. This method introduces an added stimulus for autophagy however. My solution was to use very low serum (3%) instead of complete withdrawal. It remained difficult for me to reproduce a further increase in autophagy in this model, especially over the ever-present baseline level of autophagy in NRCMs "sitting in a dish".

Engineered heart tissue (EHT) is an intriguing possibility as an *in vitro* model for cardiac hypertrophy[92]. This model allows the use of mechanical stretch as the stimulus for hypertrophy, which is the primary stimulus in pressure-overload hypertrophy. Non-myocytes such as fibroblasts, endothelial, smooth muscle cells, that are present in the heart, are found in EHTs as well. Thus the interplay between the various cells of the heart in response to hypertrophic

stimuli can be better mimicked in this model. Of course there will be technical limitations with this model as well, but I would propose that further *in vitro* studies be done in this model. I suspect that it would provide the most accurate reflection of the TAC model, the best model of cardiac hypertrophy. In this way we can better understand the role of autophagy in this process and manipulate it as a therapeutic target.

## Bibliography


1. Hill, J.A. & Olson, E.N. Cardiac plasticity. *The New England journal of medicine* **358**, 1370-1380 (2008).
2. Dorn, G.W., 2nd, Robbins, J. & Sugden, P.H. Phenotyping hypertrophy: eschew obfuscation. *Circulation research* **92**, 1171-1175 (2003).
3. Levy, D., Larson, M.G., Vasan, R.S., Kannel, W.B. & Ho, K.K. The progression from hypertension to congestive heart failure. *JAMA : the journal of the American Medical Association* **275**, 1557-1562 (1996).
4. Levy, D., Garrison, R.J., Savage, D.D., Kannel, W.B. & Castelli, W.P. Prognostic implications of echocardiographically determined left ventricular mass in the Framingham Heart Study. *N Engl J Med* **322**, 1561-1566 (1990).
5. Nakao, K., Minobe, W., Roden, R., Bristow, M.R. & Leinwand, L.A. Myosin heavy chain gene expression in human heart failure. *The Journal of clinical investigation* **100**, 2362-2370 (1997).
6. Hill, J.A. *et al.* Cardiac hypertrophy is not a required compensatory response to short-term pressure overload. *Circulation* **101**, 2863-2869 (2000).
7. Mathew, J. *et al.* Reduction of cardiovascular risk by regression of electrocardiographic markers of left ventricular hypertrophy by the angiotensin-converting enzyme inhibitor ramipril. *Circulation* **104**, 1615-1621 (2001).
8. Frey, N., Katus, H.A., Olson, E.N. & Hill, J.A. Hypertrophy of the heart: a new therapeutic target? *Circulation* **109**, 1580-1589 (2004).
9. Nemchenko, A., Chiong, M., Turer, A., Lavandero, S. & Hill, J.A. Autophagy as a therapeutic target in cardiovascular disease. *Journal of Molecular and Cellular Cardiology* **51**, 584-593 (2011).
10. Yang, Z. & Klionsky, D.J. Eaten alive: a history of macroautophagy. *Nature cell biology* **12**, 814-822 (2010).
11. Decker, R.S. & Wildenthal, K. Lysosomal alterations in hypoxic and reoxygenated hearts. I. Ultrastructural and cytochemical changes. *The American journal of pathology* **98**, 425-444 (1980).
12. Kuma, A. *et al.* The role of autophagy during the early neonatal starvation period. *Nature* **432**, 1032-1036 (2004).
13. Komatsu, M. *et al.* Impairment of starvation-induced and constitutive autophagy in Atg7-deficient mice. *The Journal of Cell Biology* **169**, 425-434 (2005).
14. Nakai, A. *et al.* The role of autophagy in cardiomyocytes in the basal state and in response to hemodynamic stress. *Nature Medicine* **13**, 619-624 (2007).
15. Zorov, D.B., Juhaszova, M. & Sollott, S.J. Mitochondrial ROS-induced ROS release: an update and review. *Biochimica et biophysica acta* **1757**, 509-517 (2006).

16. Yellon, D.M. & Hausenloy, D.J. Myocardial reperfusion injury. *N Engl J Med* **357**, 1121-1135 (2007).
17. Yan, L. *et al.* Autophagy in chronically ischemic myocardium. *Proceedings of the National Academy of Sciences of the United States of America* **102**, 13807-13812 (2005).
18. Hamacher-Brady, A., Brady, N.R. & Gottlieb, R.A. Enhancing macroautophagy protects against ischemia/reperfusion injury in cardiac myocytes. *The Journal of biological chemistry* **281**, 29776-29787 (2006).
19. Matsui, Y. *et al.* Distinct roles of autophagy in the heart during ischemia and reperfusion: roles of AMP-activated protein kinase and Beclin 1 in mediating autophagy. *Circulation research* **100**, 914-922 (2007).
20. Valentim, L. *et al.* Urocortin inhibits Beclin1-mediated autophagic cell death in cardiac myocytes exposed to ischaemia/reperfusion injury. *J Mol Cell Cardiol* **40**, 846-852 (2006).
21. Diwan, A. *et al.* Inhibition of ischemic cardiomyocyte apoptosis through targeted ablation of Bnip3 restrains postinfarction remodeling in mice. *The Journal of clinical investigation* **117**, 2825-2833 (2007).
22. Zhang, H. *et al.* Mitochondrial autophagy is an HIF-1-dependent adaptive metabolic response to hypoxia. *J Biol Chem* **283**, 10892-10903 (2008).
23. Hamacher-Brady, A. *et al.* Response to myocardial ischemia/reperfusion injury involves Bnip3 and autophagy. *Cell death and differentiation* **14**, 146-157 (2007).
24. Zhu, H. *et al.* Cardiac autophagy is a maladaptive response to hemodynamic stress. *The Journal of clinical investigation* **117**, 1782-1793 (2007).
25. Rothermel, B.A. & Hill, J.A. Autophagy in load-induced heart disease. *Circulation research* **103**, 1363-1369 (2008).
26. Williams, A. *et al.* Aggregate-prone proteins are cleared from the cytosol by autophagy: therapeutic implications. *Current topics in developmental biology* **76**, 89-101 (2006).
27. Heineke, J. & Molkentin, J.D. Regulation of cardiac hypertrophy by intracellular signalling pathways. *Nature reviews. Molecular cell biology* **7**, 589-600 (2006).
28. Klionsky, D.J. Autophagy: from phenomenology to molecular understanding in less than a decade. *Nature reviews. Molecular cell biology* **8**, 931-937 (2007).
29. Mizushima, N., Levine, B., Cuervo, A.M. & Klionsky, D.J. Autophagy fights disease through cellular self-digestion. *Nature* **451**, 1069-1075 (2008).
30. Hsu, S.C., Hazuka, C.D., Foletti, D.L. & Scheller, R.H. Targeting vesicles to specific sites on the plasma membrane: the role of the sec6/8 complex. *Trends in cell biology* **9**, 150-153 (1999).
31. Guo, W., Sacher, M., Barrowman, J., Ferro-Novick, S. & Novick, P. Protein complexes in transport vesicle targeting. *Trends in cell biology* **10**, 251-255 (2000).

32. Mostov, K.E., Verges, M. & Altschuler, Y. Membrane traffic in polarized epithelial cells. *Current opinion in cell biology* **12**, 483-490 (2000).
33. Bodemann, B.O. *et al.* RalB and the exocyst mediate the cellular starvation response by direct activation of autophagosome assembly. *Cell* **144**, 253-267 (2011).
34. Lezoualc'h, F., Métrich, M., Hmitou, I., Duquesnes, N. & Morel, E. Small GTP-binding proteins and their regulators in cardiac hypertrophy. *Journal of Molecular and Cellular Cardiology* **44**, 623-632 (2008).
35. Kawai, M. *et al.* Ral GDP dissociation stimulator and Ral GTPase are involved in myocardial hypertrophy. *Hypertension* **41**, 956-962 (2003).
36. Rockman, H.A. *et al.* Segregation of atrial-specific and inducible expression of an atrial natriuretic factor transgene in an in vivo murine model of cardiac hypertrophy. *Proc Natl Acad Sci U S A* **88**, 8277-8281 (1991).
37. Ni, Y.G. *et al.* Foxo transcription factors blunt cardiac hypertrophy by inhibiting calcineurin signaling. *Circulation* **114**, 1159-1168 (2006).
38. Livak, K.J. & Schmittgen, T.D. Analysis of relative gene expression data using real-time quantitative PCR and the 2(-Delta Delta C(T)) Method. *Methods* **25**, 402-408 (2001).
39. Nobukuni, T. *et al.* Amino acids mediate mTOR/raptor signaling through activation of class 3 phosphatidylinositol 3OH-kinase. *Proc Natl Acad Sci U S A* **102**, 14238-14243 (2005).
40. Thoreen, C.C. *et al.* An ATP-competitive mammalian target of rapamycin inhibitor reveals rapamycin-resistant functions of mTORC1. *J Biol Chem* **284**, 8023-8032 (2009).
41. Maehama, T. *et al.* RalA functions as an indispensable signal mediator for the nutrient-sensing system. *The Journal of biological chemistry* **283**, 35053-35059 (2008).
42. Voss, M. *et al.* Phospholipase D stimulation by receptor tyrosine kinases mediated by protein kinase C and a Ras/Ral signaling cascade. *J Biol Chem* **274**, 34691-34698 (1999).
43. Toschi, A. *et al.* Regulation of mTORC1 and mTORC2 complex assembly by phosphatidic acid: competition with rapamycin. *Molecular and cellular biology* **29**, 1411-1420 (2009).
44. Vega, R.B., Bassel-Duby, R. & Olson, E.N. Control of cardiac growth and function by calcineurin signaling. *J Biol Chem* **278**, 36981-36984 (2003).
45. Molkentin, J.D. *et al.* A calcineurin-dependent transcriptional pathway for cardiac hypertrophy. *Cell* **93**, 215-228 (1998).
46. Bueno, O.F. *et al.* Impaired cardiac hypertrophic response in Calcineurin Abeta -deficient mice. *Proc Natl Acad Sci U S A* **99**, 4586-4591 (2002).
47. Rothermel, B.A. *et al.* Myocyte-enriched calcineurin-interacting protein, MCIP1, inhibits cardiac hypertrophy in vivo. *Proc Natl Acad Sci U S A* **98**, 3328-3333 (2001).

48. Hill, J.A. *et al.* Targeted inhibition of calcineurin in pressure-overload cardiac hypertrophy. Preservation of systolic function. *J Biol Chem* **277**, 10251-10255 (2002).
49. Lorell, B.H. & Carabello, B.A. Left ventricular hypertrophy: pathogenesis, detection, and prognosis. *Circulation* **102**, 470-479 (2000).
50. Shiojima, I. & Walsh, K. Regulation of cardiac growth and coronary angiogenesis by the Akt/PKB signaling pathway. *Genes & development* **20**, 3347-3365 (2006).
51. DeBosch, B. *et al.* Akt1 is required for physiological cardiac growth. *Circulation* **113**, 2097-2104 (2006).
52. Condorelli, G. *et al.* Akt induces enhanced myocardial contractility and cell size in vivo in transgenic mice. *Proceedings of the National Academy of Sciences* **99**, 12333-12338 (2002).
53. Shiojima, I. *et al.* Disruption of coordinated cardiac hypertrophy and angiogenesis contributes to the transition to heart failure. *The Journal of clinical investigation* **115**, 2108-2118 (2005).
54. Aoki, M., Jiang, H. & Vogt, P.K. Proteasomal degradation of the FoxO1 transcriptional regulator in cells transformed by the P3k and Akt oncoproteins. *Proc Natl Acad Sci U S A* **101**, 13613-13617 (2004).
55. Skurk, C. *et al.* The FOXO3a transcription factor regulates cardiac myocyte size downstream of AKT signaling. *J Biol Chem* **280**, 20814-20823 (2005).
56. Sandri, M. *et al.* Foxo Transcription Factors Induce the Atrophy-Related Ubiquitin Ligase Atrogin-1 and Cause Skeletal Muscle Atrophy. *Cell* **117**, 399-412 (2004).
57. Stitt, T.N. *et al.* The IGF-1/PI3K/Akt Pathway Prevents Expression of Muscle Atrophy-Induced Ubiquitin Ligases by Inhibiting FOXO Transcription Factors. *Molecular Cell* **14**, 395-403 (2004).
58. Li, H.H. *et al.* Atrogin-1/muscle atrophy F-box inhibits calcineurin-dependent cardiac hypertrophy by participating in an SCF ubiquitin ligase complex. *The Journal of clinical investigation* **114**, 1058-1071 (2004).
59. Li, S. *et al.* Requirement for serum response factor for skeletal muscle growth and maturation revealed by tissue-specific gene deletion in mice. *Proc Natl Acad Sci U S A* **102**, 1082-1087 (2005).
60. Augusto, V., Padovani, C.R. & Campos, G.E.R. Skeletal muscle fiber types in C57BL6J mice. *Braz. J. Morphol. Sci* **21**, 89-94 (2004).
61. Cao, D.J. *et al.* Mechanical unloading activates FoxO3 to trigger Bnip3-dependent cardiomyocyte atrophy. *Journal of the American Heart Association* **2**, e000016 (2013).
62. Ogilvie, R.W. & Feeback, D.L. A metachromatic dye-ATPase method for the simultaneous identification of skeletal muscle fiber types I, IIA, IIB and IIC. *Stain technology* **65**, 231-241 (1990).
63. Seoane, J., Le, H.-V., Shen, L., Anderson, S.A. & Massagué, J. Integration of Smad and forkhead pathways in the control of

neuroepithelial and glioblastoma cell proliferation. *Cell* **117**, 211-223 (2004).
64. Molkentin, J.D. & Olson, E.N. Combinatorial control of muscle development by basic helix-loop-helix and MADS-box transcription factors. *Proceedings of the National Academy of Sciences* **93**, 9366-9373 (1996).
65. Lin, J. *et al.* Transcriptional co-activator PGC-1 alpha drives the formation of slow-twitch muscle fibres. *Nature* **418**, 797-801 (2002).
66. Zhao, J. *et al.* FoxO3 coordinately activates protein degradation by the autophagic/lysosomal and proteasomal pathways in atrophying muscle cells. *Cell metabolism* **6**, 472-483 (2007).
67. Mammucari, C. *et al.* FoxO3 controls autophagy in skeletal muscle in vivo. *Cell metabolism* **6**, 458-471 (2007).
68. Chinnadurai, G., Vijayalingam, S. & Gibson, S.B. BNIP3 subfamily BH3-only proteins: mitochondrial stress sensors in normal and pathological functions. *Oncogene* **27 Suppl 1**, S114-127 (2008).
69. Daido, S. *et al.* Pivotal role of the cell death factor BNIP3 in ceramide-induced autophagic cell death in malignant glioma cells. *Cancer research* **64**, 4286-4293 (2004).
70. Wikman-Coffelt, J., Parmley, W.W. & Mason, D.T. The cardiac hypertrophy process. Analyses of factors determining pathological vs. physiological development. *Circulation research* **45**, 697-707 (1979).
71. Lopez-Torres, M., Romero, M. & Barja, G. Effect of thyroid hormones on mitochondrial oxygen free radical production and DNA oxidative damage in the rat heart. *Molecular and cellular endocrinology* **168**, 127-134 (2000).
72. Venditti, P., Agnisola, C. & Di Meo, S. Effect of ischemia-reperfusion on heart mitochondria from hyperthyroid rats. *Cardiovascular research* **56**, 76-85 (2002).
73. Albin, R., Dowell, R.T., Zak, R. & Rabinowitz, M. Synthesis and degradation of mitochondrial components in hypertrophied rat heart. *The Biochemical journal* **136**, 629-637 (1973).
74. Kowaltowski, A.J., Castilho, R.F. & Vercesi, A.E. Opening of the mitochondrial permeability transition pore by uncoupling or inorganic phosphate in the presence of Ca2+ is dependent on mitochondrial-generated reactive oxygen species. *FEBS letters* **378**, 150-152 (1996).
75. Batandier, C., Leverve, X. & Fontaine, E. Opening of the mitochondrial permeability transition pore induces reactive oxygen species production at the level of the respiratory chain complex I. *J Biol Chem* **279**, 17197-17204 (2004).
76. Kundu, M. & Thompson, C.B. Macroautophagy versus mitochondrial autophagy: a question of fate? *Cell Death Differ* **12 Suppl 2**, 1484-1489 (2005).
77. Sohal, D.S. *et al.* Temporally regulated and tissue-specific gene manipulations in the adult and embryonic heart using a tamoxifen-inducible Cre protein. *Circulation research* **89**, 20-25 (2001).

78. Clerk, A. & Sugden, P.H. Activation of protein kinase cascades in the heart by hypertrophic G protein-coupled receptor agonists. *The American journal of cardiology* **83**, 64H-69H (1999).
79. Zhou, L.-Y. *et al.* Mitochondrial function in cardiac hypertrophy. *International Journal of Cardiology* **167**, 1118-1125 (2013).
80. Taguchi, N., Ishihara, N., Jofuku, A., Oka, T. & Mihara, K. Mitotic phosphorylation of dynamin-related GTPase Drp1 participates in mitochondrial fission. *J Biol Chem* **282**, 11521-11529 (2007).
81. Roger, V.L. *et al.* Heart disease and stroke statistics--2012 update: a report from the American Heart Association. *Circulation* **125**, e2-e220 (2012).
82. Hao, Y., Wong, R. & Feig, L.A. RalGDS couples growth factor signaling to Akt activation. *Molecular and cellular biology* **28**, 2851-2859 (2008).
83. DeBosch, B. *et al.* Akt1 is required for physiological cardiac growth. *Circulation* **113**, 2097-2104 (2006).
84. Kassiotis, C. *et al.* Markers of autophagy are downregulated in failing human heart after mechanical unloading. *Circulation* **120**, S191-197 (2009).
85. Mazure, N.M. & Pouyssegur, J. Atypical BH3-domains of BNIP3 and BNIP3L lead to autophagy in hypoxia. *Autophagy* **5**, 868-869 (2009).
86. Macpherson, P.C., Wang, X. & Goldman, D. Myogenin regulates denervation-dependent muscle atrophy in mouse soleus muscle. *Journal of cellular biochemistry* **112**, 2149-2159 (2011).
87. Li, J. & Goldberg, A. Effects of food deprivation on protein synthesis and degradation in rat skeletal muscles. *American Journal of Physiology -- Legacy Content* **231**, 441-448 (1976).
88. Baracos, V.E., DeVivo, C., Hoyle, D.H. & Goldberg, A.L. Activation of the ATP-ubiquitin-proteasome pathway in skeletal muscle of cachectic rats bearing a hepatoma. *The American journal of physiology* **268**, E996-1006 (1995).
89. Sandri, M. *et al.* PGC-1alpha protects skeletal muscle from atrophy by suppressing FoxO3 action and atrophy-specific gene transcription. *Proc Natl Acad Sci U S A* **103**, 16260-16265 (2006).
90. Sadoshima, J. & Izumo, S. The cellular and molecular response of cardiac myocytes to mechanical stress. *Annual review of physiology* **59**, 551-571 (1997).
91. Andrés, V. & Walsh, K. Myogenin expression, cell cycle withdrawal, and phenotypic differentiation are temporally separable events that precede cell fusion upon myogenesis. *The Journal of cell biology* **132**, 657-666 (1996).
92. Hirt, M.N., Hansen, A. & Eschenhagen, T. Cardiac Tissue Engineering State of the Art. *Circulation research* **114**, 354-367 (2014).